Articles

Synthesis and Structure–Activity Relationships of Substituted 1,4-Dihydroquinoxaline-2,3-diones: Antagonists of *N*-Methyl-D-aspartate (NMDA) Receptor Glycine Sites and Non-NMDA Glutamate Receptors

John F. W. Keana,*,† Sunil M. Kher,† Sui Xiong Cai,‡ Christian M. Dinsmore,† Anne G. Glenn,† J. Guastella,‡ Jin-Cheng Huang,‡ Victor Ilyin,‡,|| Yixin Lü,† Pamela L. Mouser,† Richard M. Woodward,‡ and Eckard Weber*,§

Department of Chemistry, University of Oregon, Eugene, Oregon 97403, Acea Pharmaceuticals Inc., A Subsidiary of CoCensys, Inc., 213 Technology Drive, Irvine, California 92718, and Department of Pharmacology, University of California, Irvine, California 92717

Received May 15, 1995®

A series of mono-, di-, tri-, and tetrasubstituted 1,4-dihydroquinoxaline-2,3-diones (QXs) were synthesized and evaluated as antagonists at *N*-methyl-D-aspartate (NMDA)/glycine sites and α-amino-3-hydroxy-5-methylisoxazole-4-propionic acid-preferring non-NMDA receptors. Antagonist potencies were measured by electrical assays in *Xenopus* oocytes expressing rat whole brain poly(A)$^+$ RNA. Trisubstituted QXs **17a** (ACEA 1021), **17b** (ACEA 1031), **24a**, and **27**, containing a nitro group in the 5 position and halogen in the 6 and 7 positions, displayed high potency (K_b ~ 6–8 nM) at the glycine site, moderate potency at non-NMDA receptors (K_b = 0.9–1.5 μM), and the highest (120–250-fold) selectivity in favor of glycine site antagonism over non-NMDA receptors. Tetrasubstituted QXs **17d,e** were more than 100-fold weaker glycine site antagonists than the corresponding trisubstituted QXs with F being better tolerated than Cl as a substituent at the 8 position. Di- and monosubstituted QXs showed progressively weaker antagonism compared to trisubstituted analogues. For example, removal of the 5-nitro group of **17a** results in a ~100-fold decrease in potency (**10a,b,z**), while removal of both halogens from **17a** results in a ~3000-fold decrease in potency (**10v**). In terms of steady-state inhibition, most QX substitution patterns favor antagonism at NMDA/glycine sites over antagonism at non-NMDA receptors. Among the QXs tested, only **17i** was slightly selective for non-NMDA receptors.

Introduction

N-Methyl-D-aspartate (NMDA) receptors are implicated in the pathology of numerous neurodegenerative disorders, including the acute brain damage which follows ischemic stroke and the more gradual loss of neurons associated with epilepsy, Alzheimer's disease, and acquired immune deficiency syndrome (AIDS)-related dementia.[1] In each case, neuronal damage is thought to be a consequence of the "excitotoxic" effects of glutamate, wherein excessive excitatory input causes pathological increases in intracellular Ca^{2+} and ultimately cell death.[2]

In terms of therapeutic intervention, there are at least four sites for antagonism of NMDA receptors:[3] (i) phencyclidine (PCP)-binding sites, located within the channel lumen and accessible in open-channel configurations,[4] (ii) glutamate-binding sites, where antagonists compete with glutamate to inhibit channel activity,[5] (iii) glycine coagonist sites, which must be occupied by glycine for glutamate to gate the channel,[6] and (iv) polyamine inhibitory sites.[7] Numerous studies have shown that PCP site ligands such as dizocilpine (MK-801) and glutamate site antagonists such as CGS 19755, LY 274614, and [3-((±)-2-carboxypiperazin-4-yl)prop-1-yl]phosphonic acid (CPP) have neuroprotective actions in animal models of stroke.[8] Unfortunately, the clinical potential of these classes of antagonists can be compromised by psychotomimetic side effects.[9,10] For reasons that remain uncertain, the behavioral side effect profiles of glycine site antagonists are more encouraging.[10–12] In addition, glycine site antagonists do not appear to cause neuronal vacuolization, a pathological phenomenon observed following treatment with potent PCP site ligands and competitive antagonists.[13]

A wide variety of glycine site antagonists are now known.[14] Among the more potent series are (i) the kynurenic acids, which include 7-chloro-5-iodo-kynurenic acid (IC_{50} in binding studies, ~30 nM) (**1**),[15] (ii) the 2-carboxytetrahydroquinolines, which include (±)-*trans*-2-carboxy-5,7-dichloro-4-(phenylureido)tetrahydroquinoline (IC_{50} ~ 8 nM) (**2**),[16] (iii) the tricyclic 1,4-dihydroquinoxaline-2,3-diones (QXs), which include (*S*)-9-bromo-5-[(phenylcarbamoyl)methyl]-6,7-dihydro-1*H*,5*H*-pyrido[1,2,3-*de*]QX (K_i = 0.96 nM) (**3**),[17] (iv) the benzazepines, which include 8-methyl-2,5-dihydro-2,5-dioxo-3-hydroxy-1*H*-benzazepine (K_b ~ 470 nM) (**4**),[18] and (v) the 3-substituted-4-hydroxyquinolin-2(1*H*)-ones, which include 3-(3-phenoxyphenyl)-4-hydroxyquinolin-2(1*H*)-one (IC_{50} ~ 2 nM) (**5**).[19]

Blood–brain barrier penetration, one indication of *in vivo* bioavailability, varies drastically both between and

* Authors to whom correspondence should be addressed.
† University of Oregon.
‡ Acea Pharmaceuticals Inc.
§ University of California.
|| Permanent address: Institute of Cell Biophysics, Russian Academy of Sciences, Pushchino, Moscow Reg. 142292, Russia.
® Abstract published in *Advance ACS Abstracts*, October 1, 1995.

0022-2623/95/1838-4367$09.00/0

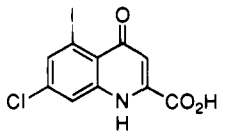

1

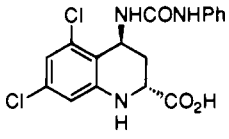

2

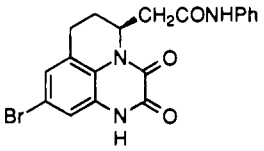

3

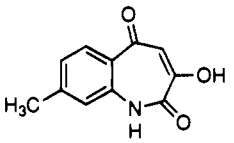

4

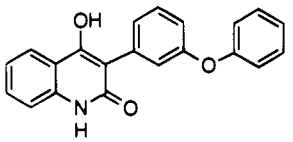

5

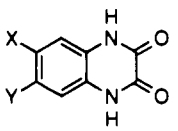

6, X = Y = H
6a, X = Y = NO_2
6b, X = CN, Y = NO_2

within the different classes of antagonists. For example, kynurenic acids and 2-carboxytetrahydroquinolines are largely inactive in rodents following systemic administration, whereas some 3-phenyl-4-hydroxyquinolin-2(1*H*)-ones have anticonvulsant effects at oral doses as low as 1 mg/kg.[19]

QXs **6a,b** were initially reported as selective antagonists at α-amino-3-hydroxy-5-methylisoxazole-4-propionic acid (AMPA)-preferring non-NMDA receptors.[20] Subsequent characterization revealed that the pharmacological profile of these compounds also includes moderately potent antagonism at NMDA receptor glycine sites.[21] Herein, we report the chemistry and pharmacology of a series of QXs with novel substitution patterns on the benzene ring. The steady-state inhibitory potencies of these molecules were measured at rat brain NMDA and non-NMDA receptors expressed in *Xenopus* oocytes. Several trisubstituted compounds were found to be potent and selective glycine site antagonists. One of these is ACEA 1021 (**17a**), a neuroprotective drug currently undergoing clinical trials for stroke. A preliminary report describing some of these results has appeared previously.[22]

Chemistry

Synthesis. Table 1 lists the compounds that have been synthesized together with supporting data. QX **6** was commercially available, while QXs **10** (Scheme 1) were prepared by condensation of diethyl oxalate[23] or, better, oxalic acid[24] with the corresponding 1,2-diaminobenzenes **9**. When **9**s were not commercially available, they were prepared from **8** by one of several methods. Treatment of the appropriate 2-nitroanilines **8** with tin(II) chloride dihydrate in refluxing ethanol or ethyl acetate furnished **9**,[25] as did agitating solutions of **8** in methanol with Pd/C under hydrogen gas. A different procedure was used in the case of the symmetrically substituted 2,6-dinitroaniline **8u**. Selective reduction to **9u** was achieved by treatment with a refluxing solution of ammonium sulfide in ethanol and water.[26] When nitroanilines **8** were not commercially available, they were prepared from the requisite anilines **7** employing routine protection–deprotection sequences (Scheme 1).

QXs **10x,y** are known[27] and were prepared by chlorination and bromination, respectively, of commercially available QX **6**. **10z** was prepared by chlorination of **10y** (Scheme 2).

A third approach (Scheme 3) for the synthesis of QXs utilized selenium heterocycles to produce the 5-nitro QXs **16**. Regiospecific nitration of selenium heterocycles of type **13b** is known to furnish **14b**.[28] Accordingly, the nitroaniline **11b** was reduced to the corresponding diamine **12b**, which was then allowed to react with selenium oxide in aqueous ethanol, giving (2,1,3)benzoselenadiazole **13b**. Treating **13b** with a mixture of nitric acid and sulfuric acid gave **14b**, which was then converted to the corresponding 1,2-diamine **15b** with hydriodic acid. Finally, **15b** was condensed with oxalic acid to give **16b**. A similar reaction sequence was followed using **11a,c** to give **16a,c**, respectively. Bromination[29] of **16b** gave **27** (Table 1). All the compounds described in Scheme 3 were assigned the structures shown based on the ^{1}H NMR spin-spin splitting pattern and coupling constants observed for their aromatic protons.

Nitration (KNO_3, H_2SO_4 or KNO_3, TFA) of QXs **10a–h**, **6**, and **10n,x** furnished **17a–h,i,n,x**, respectively (Scheme 4). KNO_3/TFA was the reagent combination of choice when **10**s were substituted with two or more fluorine atoms on the aromatic ring. **17x** was further nitrated (KNO_3, H_2SO_4) to **18x**. Nitro QXs **17a–c** were reduced with tin(II) chloride dihydrate to the corresponding amino QXs **18a–c**. Further, **18a** was acetylated with acetyl chloride to give **19**.

Nitration of unsymmetrically 6,7-disubstituted QXs was not satisfactory in many instances using conventional nitration procedures described in Scheme 4. While nitration of **10f,g** gave the single nitro isomers, other nitrations produced mixtures of two isomers that were difficult to separate. Hence it was necessary to develop a regiospecific procedure to prepare 5-nitro-6,7-disubstituted QXs **24a–d** (Scheme 5).

The approach is based on the observation that treatment of 3,4-dihydroquinoxalin-2(1*H*)-ones **23** with excess fuming nitric acid (10–20 equiv) in TFA results both in nitration exclusively at the 5 position and in oxidation to the QXs **24**.[30] Accordingly, fluorobenzenes **20** were converted into *N*-phenyl glycinates **22**. Reduction of **22** and concomitant cyclization gave quinoxalin-2(1*H*)-ones **23**. Finally, treatment of **23** with excess fuming HNO_3 in TFA gave analytically pure QXs **24**.

QXs **26a,b** (Scheme 6) were prepared by reduction of the nitro QXs **17c',n** to amino QXs **25a,b** respectively, followed by diazotization and subsequent treatment with copper(I) chloride in hydrochloric acid.

Structural Considerations. Structures of the synthetic intermediates and tested ligands were assigned by applying well-established ortho-, para-, or meta-directing effects of substituents already present on the aromatic ring and are consistent with ^{1}H NMR spectra and elemental composition by HRMS. In the case of the F-containing QXs, structures were confirmed by the magnitude of the F-H coupling constant (*J*) in the ^{1}H NMR spectra.[31] Structures of the corresponding Cl or

Table 1. Physical Data, NMR Spectroscopic Data, and Methods of Preparation for Substituted QXs

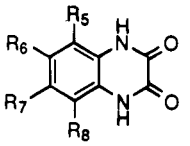

compd no.	R_5	R_6	R_7	R_8	mp (°C)	starting material; methods[a]	yield (%)	formula[b]	^{1}H NMR[c]
6	H	H	H	H	>300	comm available			
10a	H	Cl	Cl	H	>400[d]	**9a**; H	74		7.23 (2H), 12.02 (2H)
10b	H	Br	Br	H	335[e]	**7b**; B, E, H	49		7.37 (2H), 11.96 (2H)
10c	Cl	H	CF_3	H	346–348	**8c**; G	36	$C_9H_4ClF_3N_2O_2$[f]	7.30, 7.53, 11.9 (b, 2H)
10d	Cl	Cl	Cl	H	355	**8d**; D, G	23	$C_8H_3Cl_3N_2O_2$[f]	7.25, 11.62, 12.12
10e	F	Cl	F	H	>250	**7e**; B, D, H	62	$C_9H_3ClF_2N_2O_2$	6.93 (d, J = 9.6), 12.14, 12.17 (b)
10f	H	Br	CF_3	H	>360	**7f**; A, D, H	46	$C_9H_4BrF_3N_2O_2$[f]	7.54, 7.74, 12.05, 12.30
10g	H	Cl	CF_3	H	>360	**7g**; A, D, H	13	$C_9H_4ClF_3N_2O_2$[f]	7.27, 7.48, 12.14 (2H)
10h	H	F	F	H	>360	**8h**; E, H	89	$C_8H_4F_2N_2O_2$[f]	7.05 (d, J = 9.3), 11.94 (2H)
10i	Br	Cl	Cl	H	332–335	**8i**; D, G	24	$C_8H_3BrCl_2N_2O_2$	7.30, 11.19 (b), 12.14 (b)
10j	Br	H	Br	H	356–358	**8j**; D, G	16	$C_8H_4Br_2N_2O_2$[f]	7.21 (d, J = 2.1), 7.53 (d, J = 2.1), 11.1 (b), 12.1 (b)
10k	Br	H	CF_3	H	332–334	**9k**; G	62	$C_9H_4BrF_3N_2O_2$[f]	7.28, 7.56, 11.7 (b, 2H)
10l	CF_3	H	Br	H	307–309	**7l**; A, D, H	22	$C_9H_4BrF_3N_2O_2$[f]	7.51 (d, J = 1.8), 7.56 (d, J = 1.5), 11.34, 12.22
10m	CF_3	H	CF_3	H	308–310[g]	**7m**; A, D, H	12	$C_{10}H_4F_6N_2O_2$[f]	7.65, 7.69, 11.58, 12.31
10n	CF_3	H	Cl	H	302–304	**7n**; A, D, H	31	$C_9H_4ClF_3N_2O_2$[f]	7.37 (d, J = 1.8), 7.47 (d, J = 1.8), 11.35, 12.22
10o	CF_3	H	F	H	300–302	**7o**; A, D, H	9	$C_9H_4F_4N_2O_2$[f]	7.18 (dd, J = 8.7, 2.7), 7.36 (d, J = 8.7, 2.7), 11.27, 12.24
10p	Cl	H	Cl	H	326–328[h]	**9p**; D, G	41		7.05 (d, J = 1.8), 7.32 (d, J = 1.8), 11.5 (b), 12.1 (b)
10q	F	F	F	F	330–331[i]	**8q**; D, G	46	$C_8H_2F_4N_2O_2$[f]	12.33 (b, 2H)
10r	F	F	F	H	>360	**7r**; B, D, H	9	$C_8H_3F_3N_2O_2$	6.91 (m), 12.02, 12.19
10s	H	F	CF_3	H	330–333	**7s**; A, D, H	20	$C_9H_4F_4N_2O_2$[f]	7.08 (d, J = 11.4), 7.38 (d, J = 5.1), 12.02, 12.23
10t	NO_2	H	Cl	H	315–317[j]	**8t**; F, H	52	$C_8H_4ClN_3O_4 \cdot 0.5H_2O$	7.40, 7.90, 11.19, 12.34
10u	H	Cl	F	H	344–348	**9u**; G	45	$C_8H_4ClFN_2O_2$[f]	6.93 (d, J = 10.2), 7.08 (d, J = 7.2)
10v	NO_2	H	H	H	279–283[k]	**9v**; H	77		7.26 (t, J = 8.1), 7.46 (d, J = 7.8), 7.87 (dd, J = 8.4, 0.9), 11.09, 12.31
10w	Cl	F	F	H	322–326	**8h**; P, D, G	8	$C_8H_3ClF_2N_2O_2$[f,l]	7.05 (dd, J = 10.8, 7.2), 11.6 (b, 2H)
10x	H	Cl	H	H	>360[m]	**6**; P	29		7.07 (m, 3H), 11.94 (2H)
10y	H	Br	H	H	>350[m]	**6**; P	53		7.04 (d, J = 9), 7.24 (m, 2H), 11.96 (b, 2H)
10z	H	Br	Cl	H	>360	**10y**; P	42	$C_8H_4BrClN_2O$[f]	7.24, 7.37, 11.8, 12.2
16a	NO_2	H	CF_3	H	329–332[n]	**11a**; I	22	$C_9H_4F_3N_3O_4$	7.64, 8.11, 11.41, 12.43
16b	NO_2	Cl	H	H	321	**11b**; I	23	$C_8H_4ClN_3O_4$[f]	7.22 (d, J = 9.0), 7.36 (d, J = 8.7), 12.14, 12.22
16c	NO_2	Br	H	H	>350	**11c**; I	36	$C_8H_4BrN_3O_4$[o]	7.15 (d, J = 8.7), 7.47 (d, J = 8.7), 12.12 (b), 12.22
17a	NO_2	Cl	Cl	H	342–344	**10a**; J	90	$C_8H_3Cl_2N_3O_4$	7.38, 12.28, 12.37 (b)
17b	NO_2	Br	Br	H	352–354	**10b**; J	77	$C_8H_3Br_2N_3O_4$[f]	7.48, 12.22, 12.26
17c	Cl	H	CF_3	NO_2	305	**10c**; J	14	$C_9H_3ClF_3N_3O_4$[f]	7.86, 12.03, 12.43 (b)
17c′	Cl	NO_2	CF_3	H	345	**10c**; J	70	$C_9H_3ClF_3N_3O_4$[f]	7.48, 12.21, 12.42
17d	NO_2	Cl	Cl	Cl	324	**10d**; J	65	$C_8H_2Cl_3N_3O_4$[f]	11.9 (b), 12.5 (b)
17e	NO_2	F	Cl	F	310	**10e**; K	7	$C_8H_2ClF_2N_3O_4$	12.10 (b), 12.50
17f	NO_2	Br	CF_3	H	333–335	**10f**; J	74	$C_9H_3BrF_3N_3O_4$[f]	7.61, 12.34, 12.60 (b)
17g	NO_2	Cl	CF_3	H	342–345	**10g**; J	80	$C_9H_3ClF_3N_3O_4$	7.62, 12.35
17h	NO_2	F	F	H	288–290	**10h**; K	68	$C_8H_3F_2N_3O_4$	7.33, 11.86, 12.25
17i	H	NO_2	H	H	>300	**6**; J	78	$C_8H_5N_3O_4$[p]	7.21 (d, J = 8.7), 7.92 (m, 2H), 12.14 (b, 1H), 12.33 (b, 1H)
17n	CF_3	NO_2	Cl	H	278–280	**10n**; J	91	$C_9H_3ClF_3N_3O_4$[f]	7.53, 11.8 (b), 12.46
17x	H	Cl	NO_2	H	>370	**10x**; J	37	$C_8H_4ClN_3O_4$[f]	7.25, 7.8, 12.18, 12.30
18a	NH_2	Cl	Cl	H	>360	**17a**; L	62	$C_8H_5Cl_2N_3O_2$	5.94 (2H), 6.60, 11.32, 11.87
18b	NH_2	Br	Br	H	324–326	**17 b**; L	59	$C_8H_5Br_2N_3O_2$[f]	5.84 (2H), 6.73, 11.26, 11.81
18c	Cl	H	CF_3	NH_2	>360	**17c**; L	93	$C_9H_5ClF_3N_3O_2$[f]	5.92 (2H), 7.24, 11.32, 11.44
18x	NO_2	NO_2	Cl	H	298–300	**17x**; J	35	$C_8H_3ClN_4O_6$[f]	7.75, 10.82, 11.53
19	NHAc	Cl	Cl	H	320–322	**18a**; M	88	$C_{10}H_7Cl_2N_3O_3$[f]	2.06 (3H), 7.24, 9.62, 11.66, 12.10
24a	NO_2	Br	Cl	H	338–343	**20a**; N	26	$C_8H_3BrClN_3O_4$	7.35, 12.25 (2H)
24b	NO_2	Br	F	H	323–327	**20 b**; N	11	$C_8H_3BrFN_3O_4$	7.18 (d, J = 9.0), 12.21, 12.32
24c	NO_2	F	Br	H	316–321	**20c**; N	5	$C_8H_3BrFN_3O_4$	7.46 (d, J = 6.3), 12.01 (b), 12.18
24d	NO_2	F	Cl	H	308–310	**20d**; N	8	$C_8H_3ClFN_3O_4 \cdot H_2O$	7.37 (d, J = 6.9), 12.02 (b), 12.22
26a	Cl	Cl	CF_3	H	>250	**17c′**; L, O	52	$C_9H_3Cl_2F_3N_2O_2$[f]	7.49, 11.85, 12.22
26b	CF_3	Cl	Cl	H	305–307	**17n**; L, O	69	$C_9H_3Cl_2F_3N_2O_2$[f]	7.52, 11.05 (b), 12.27
27	NO_2	Cl	Br	H	>350	**16b**; P	44	$C_8H_3BrClN_3O_4$[f]	7.48, 12.22, 12.32 (b)

[a] For details of synthesis, refer to experimentals. [b] Analyses for C, H, and N are within ±0.4% of the theoretical values, unless otherwise noted. [c] Unless otherwise noted, values listed are for one-proton singlets. Abbreviations: b = broad singlet, d = doublet, dd = double doublet, m = multiplet, and t = triplet. Splitting values are reported in hertz (Hz). [d] Lit.[23] mp >360 °C. [e] Lit.[23] mp >360 °C. [f] HRMS ± 0.002, purity by HPLC, >95.0%. [g] Lit.[44] mp 333 °C. [h] Lit.[45] mp 320 °C. [i] Lit.[46] mp 300 °C. [j] Lit.[44] mp 320–323 °C. [k] Lit.[44] mp 284–285 °C. [l] Contaminated by 11% dechloro QX. [m] See ref 27. [n] Lit.[44] mp 342–344 °C. [o] Contaminated by 5% debromo QX. [p] See ref 23.

Scheme 1[a]

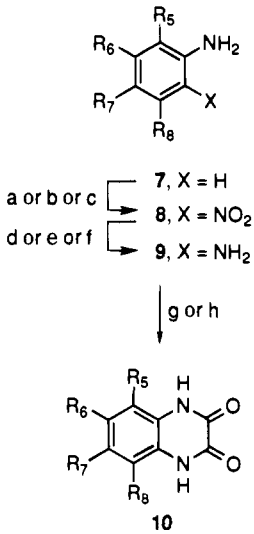

	R_5	R_6	R_7	R_8
a,	H	Cl	Cl	H
b,	H	Br	Br	H
c,	Cl	H	CF_3	H
d,	Cl	Cl	Cl	H
e,	F	Cl	F	H
f,	H	Br	CF_3	H
g,	H	Cl	CF_3	H
h,	H	F	F	H
i,	Br	Cl	Cl	H
j,	Br	H	Br	H
k,	Br	H	CF_3	H
l,	CF_3	H	Br	H
m,[l]	H	CF_3	H	CF_3
n,	CF_3	H	Cl	H
o,	CF_3	H	F	H
p,	Cl	H	Cl	H
q,	F	F	F	F
r,	F	F	F	H
s,	H	F	CF_3	H
t,	NO_2	H	Cl	H
u,	H	Cl	F	H
v,	NO_2	H	H	H
w,	Cl	F	F	H

[a] Reagents: (a) i. Ac_2O, ii. HNO_3, H_2SO_4, iii. HCl; (b) i. Ac_2O, $CHCl_3$, ii. KNO_3, H_2SO_4; (c) i. $(CF_3CO)_2O$, ii. HNO_3, H_2SO_4, iii. K_2CO_3, MeOH; (d) $SnCl_2 \cdot 2H_2O$, EtOH or EtOAc; (e) Pd/C, EtOH; (f) $(NH_4)_2S$, aqueous EtOH; (g) $(COOEt)_2$; (h) $(COOH)_2 \cdot 2H_2O$, 2 N HCl; (i) same as **10m**, Table 1.

Scheme 2[a]

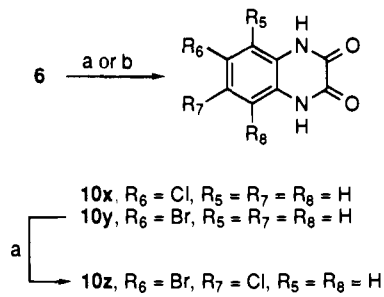

[a] Reagents: (a) NCS, DMF; (b) NBS, DMF.

Br compounds were assigned by analogy to the fluorine derivatives.

The structures of 6,7-dichloro-1,4-dihydro-5-nitroquinoxaline-2,3-dione (**17a**), 7-chloro-5-(trifluoromethyl)-1,4-dihydro-6-nitroquinoxaline-2,3-dione (**17n**), and 5-chloro-7-(trifluoromethyl)-1,4-dihydro-6-nitroquinoxaline-2,3-dione (**17c'**) were established by single-crystal X-ray crystallographic determinations (see supporting information). The X-ray studies indicated that in all three QXs, the nitro group is twisted out of the plane of the aromatic ring.

Biology

Potencies of QXs at mammalian NMDA and AMPA-preferring non-NMDA receptors were assessed by electrical assays in *Xenopus* oocytes expressing rat whole brain poly(A)$^+$ RNA. NMDA receptors were selectively activated by coapplication of NMDA and glycine.[6] Membrane current responses elicited by NMDA/glycine were inward at a holding potential of −70 mV, showing an initial spike of current and a subsequent more slowly developing peak. For all pharmacological assays the spike of current, due to secondary activation of Ca^{2+}-gated Cl^- channels,[32] was ignored and response amplitudes were measured at the peak of the second phase (e.g., Figure 1, arrow). Non-NMDA receptors expressed in oocytes by rat brain mRNA are predominantly

Scheme 3[a]

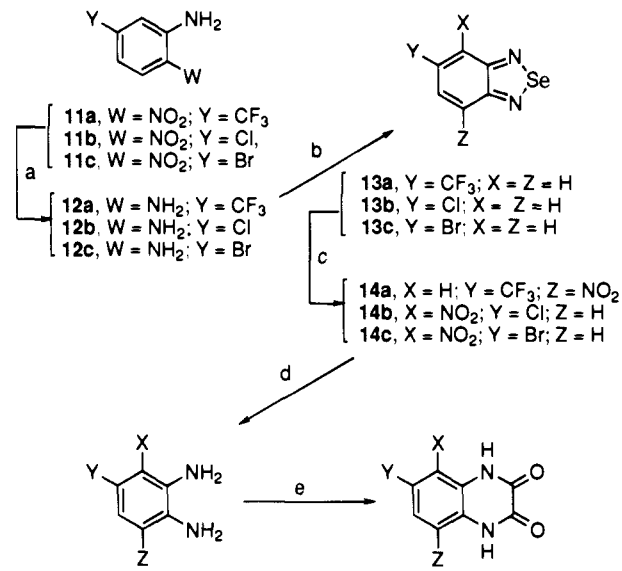

[a] Reagents: (a) $SnCl_2 \cdot 2H_2O$ in EtOH; (b) SeO_2, aqueous EtOH; (c) HNO_3, H_2SO_4; (d) 48% HI; (e) $(COOH)_2 \cdot 2H_2O$, 2 N HCl.

Scheme 4[a]

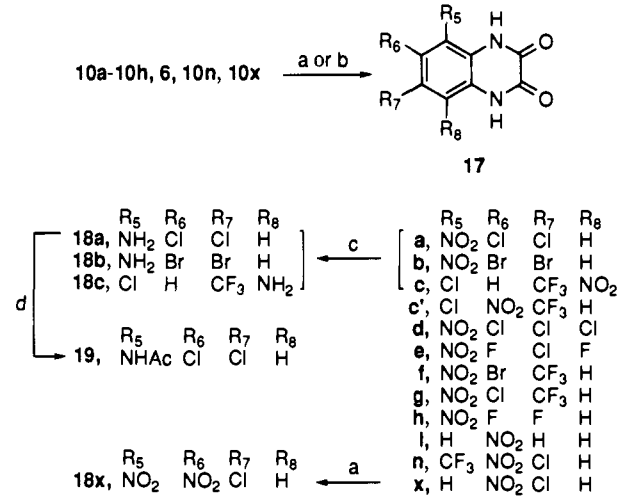

[a] Reagents: (a) KNO_3, H_2SO_4; (b) HNO_3, TFA; (c) $SnCl_2 \cdot 2H_2O$ in EtOH or EtOAc; (d) AcCl.

AMPA-preferring subtypes. The AMPA receptors were activated by application of kainic acid, which elicits non-desensitizing responses and hence larger steady-state currents than AMPA. The membrane currents were inward at −70 mV and had a monophasic time course (not illustrated).[33-35]

Apparent agonist affinities (EC_{50}s) were estimated from concentration−response curves (Figure 1). For NMDA receptor ligands, glycine receptor affinity was measured at a fixed concentration of 100 μM NMDA, and NMDA receptor affinity was measured using 10 μM glycine. Current ranges and mean maximum responses in concentration−response experiments for glycine, NMDA, and kainic acid were 367−740 nA (527 ± 59 nA, $n = 6$), 420−790 nA (569 ± 99 nA, $n = 4$), and 1040−2925 nA (1932 ± 668 nA, $n = 3$), respectively. Levels of receptor expression were similar for assays of antagonist potency.

Scheme 5[a]

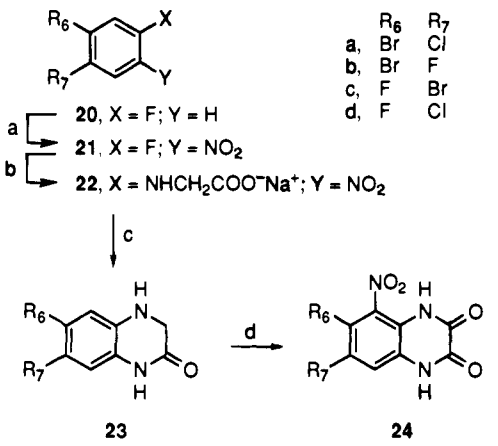

[a] Reagents: (a) KNO_3, H_2SO_4; (b) $NH_2CH_2COO^-Na^+$, DMF, H_2O; (c) $SnCl_2 \cdot 2H_2O$, EtOH; (d) fuming HNO_3, TFA.

Scheme 6[a]

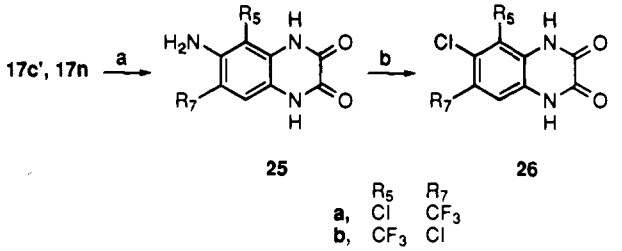

[a] Reagents: (a) $SnCl_2 \cdot 2H_2O$, EtOH; (b) concentrated HCl, $NaNO_2$, CuCl.

IC_{50} values of QXs at NMDA receptor glycine sites and non-NMDA receptors were estimated from partial (three- or four-point) concentration–inhibition curves (e.g., Figure 2). Oocytes were pretreated with antagonist for ~30 s prior to receptor activation, and inhibition was fully washed out following 1–5 min of wash. Antagonist concentrations were selected such that levels of inhibition ranged between ~20% and 80%, i.e., within the pseudolinear portion of semilog plots and spanning the IC_{50} value. Fixed agonist concentrations were 1 μM glycine (~80% saturating)/100 μM NMDA for NMDA receptors and 20 μM kainate (~10% saturating) for non-NMDA receptors. For the majority of compounds, slope values for concentration–inhibition curves ranged between −1.3 and −0.9. Compounds showing potentially atypical slopes were **17x**, **19**, **10m**, and **18x**, slope > −0.9 in NMDA assays, **6** and **16b**, slope > −0.9 in non-NMDA assays, **10i**,**d**,**r**, **16c**, and **26b**, slope < −1.3 in NMDA assays, and **10j**,**n** and **17b**,**g**, slope < −1.3 in non-NMDA assays. These groups of compounds do not share any common motifs with respect to substitution patterns. We suspect that the main source of variability in slope values stems from the narrow range of antagonist concentrations used in the partial curves, though the possibility that some compounds detect a pharmacologically heterogeneous population of receptors cannot be wholly ruled out. The pharmacology of **17a**,**b** and **10d** was characterized in detail, and antagonism at NMDA glycine sites and non-NMDA receptors was found to be full and consistent with a competitive mechanism (presented elsewhere[35]). Antagonist dissociation constants (K_b values) for all the QXs tested in the present study were estimated by assuming full competitive antagonism and applying a Leff–Dougall variant of the Cheng–Prussoff relationship (Table 2).[36] Steady-state

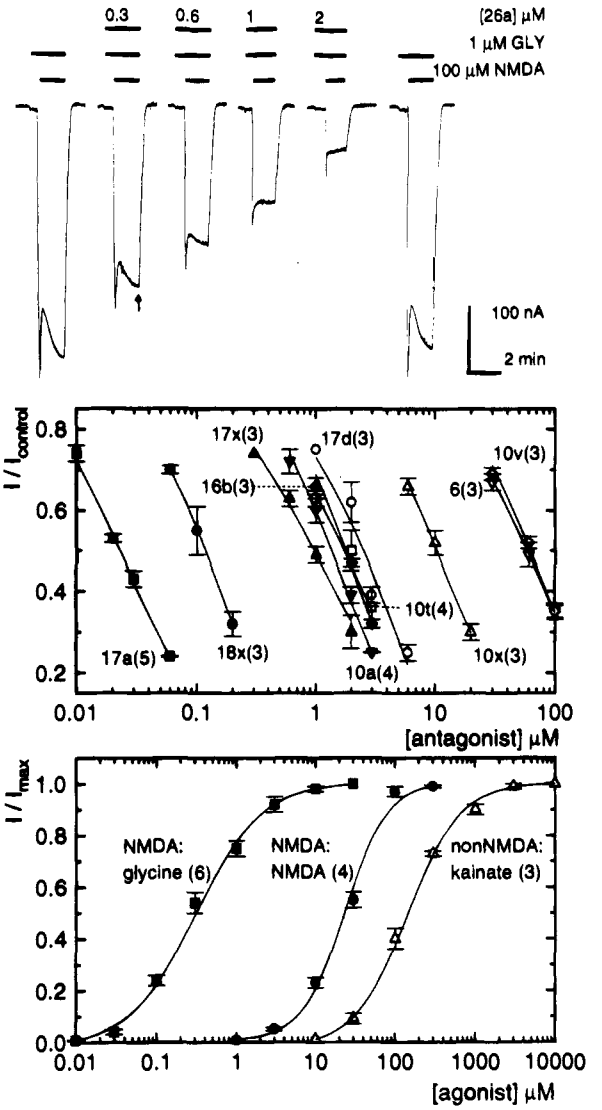

Figure 1. Upper panel: Sample records illustrating measurement of a partial concentration–inhibition curve for QX **26a** at rat brain NMDA receptors expressed in an oocyte. **26a** caused a dose-dependent reduction in current. Amplitudes were measured at the slow or plateau phase of the response (arrow). Antagonists were applied together with glycine to promote equilibration prior to receptor activation. Middle panel: Partial concentration–inhibition curves comparing potencies of nitro-/chloro-substituted QXs at NMDA receptors (glycine = 1 μM, NMDA = 100 μM). This series shows a ~2000-fold range in IC_{50} values. Broken lines, **16b** (◆) and **10t** (□) have almost identical IC_{50} values. Data are plotted as the mean ± SEM expressed as a fraction of control response (number of experiments is given in parentheses). Smooth curves, best fits of eq 2 to data for each antagonist. Optimal IC_{50} (in μM) and slope values for fits are 0.024, −1.01 for **17a**; 0.17, −1.1 for **18x**; 1.1, −0.86 for **17x**; 1.6, −1.2 for **10a**; 2.0, −1.3 for **16b**; 2.1, −0.98 for **10t**; 5.4, −0.91 for **17d**; 11, −1.3 for **10x**; 68, −1.1 for **6**; and 71, −1.2 for **10v** (quoted to two significant figures). Lower panel: Concentration–response curves for glycine at NMDA receptors, NMDA at NMDA receptors, and kainic acid at AMPA-preferring non-NMDA receptors. Smooth curves, best fits of eq 1 to data for each drug (see the Experimental Section). Optimal EC_{50} and slope values for these fits are 0.3 μM, 1.1 for glycine; 24 μM, 1.6 for NMDA; and 140 μM, 1.3 for kainic acid.

selectivity indices for glycine site antagonism were estimated by dividing K_b at non-NMDA receptors by K_b at glycine sites.

Binding studies with **17a**,**b** and **10d** indicated weak affinity at NMDA glutamate-binding sites. (Inhibition

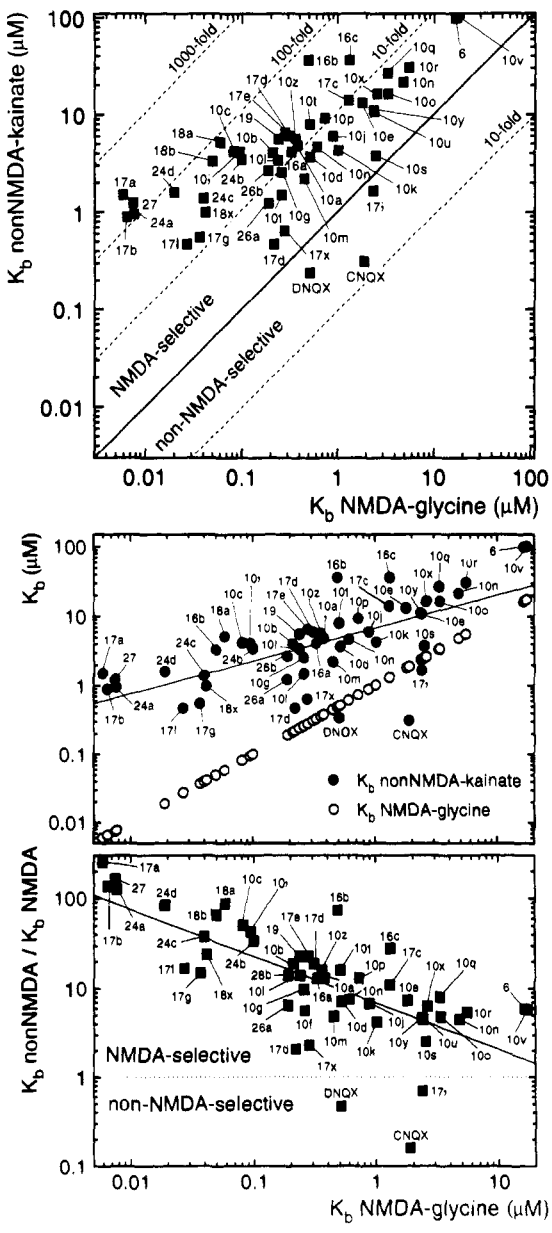

Figure 2. Upper panel: K_b values at non-NMDA receptors plotted as a function of K_b values at NMDA receptor glycine sites (data from Table 2). Apparent affinities are plotted on symmetrical axes. The solid line bisects the graph into equal areas defining selectivity for NMDA receptor glycine sites or AMPA-preferring non-NMDA receptors. Parallel broken lines indicate levels of selectivity in each area. Under steady-state conditions, the vast majority of QXs assayed in this study show selectivity for glycine sites. K_b values for DNQX and CNQX were measured in separate studies employing similar procedures[35] and are included for purposes of comparison. Middle panel: Relationship between potency at NMDA receptor glycine sites and potency at non-NMDA receptors. Increased potency at glycine sites generally correlates with an increase in potency at non-NMDA receptors. Solid line, the apparent linear fit of all data points for non-NMDA receptors; slope value is 0.48. K_b values for glycine sites are included for direct comparison. Equation used for the fit: y scale (Y) = (0.83 ± 0.071) + (0.48 ± 0.074)x scale (X); correlation coefficient, R = 0.67. Lower panel: Relationship between potency at NMDA receptor glycine sites and selectivity of antagonism with respect to non-NMDA receptors. Increase in potency at glycine sites generally correlates with an increase in selectivity. Solid line is the apparent linear fit of all selectivity indices; slope value is −0.52. Equation used for the fit: y scale (Y) = (0.84 ± 0.072) − (0.52 ± 0.075)x scale (X); R = 0.70.

of [^{3}H]CGS 17955 binding indicated K_is > 50 μM; E. Weber, unpublished results.) This is consistent with previous studies suggesting that QXs as a class have low potency as conventional competitive antagonists at NMDA receptors.[21] In the present study, electrophysiological assays for glutamate site antagonism were designed simply to assess some upper limits of potency. Agonist concentrations were 1 mM glycine, promoting saturation at glycine sites, and 1−5 μM NMDA, to maximize chances of detecting inhibition at glutamate-binding sites. Any strychnine-sensitive glycine responses, coexpressed by the whole brain poly(A)$^+$ RNA, were allowed to desensitize, and the steady-state level was used as a base line for assaying effects at NMDA receptors. Assuming a competitive interaction, minimum K_b values were estimated using the EC_{50} and slope value for NMDA (Figure 1) and the highest concentration of antagonist that failed to induce 50% inhibition of the response.[36] In this type of functional assay, defining potency limits at glutamate sites was compromised by the encroachment of glycine site antagonism and the limited solubility of most QXs at high micromolar concentrations. As a result, demonstrable selectivity indices were progressively reduced as glycine site potency decreased. For example, QXs with glycine site K_bs of <0.01, 0.01−0.1, and 0.1−1 μM showed glutamate site K_bs of >5 (>500-fold selectivity), >18 (>180-fold selectivity), and >50 (>50-fold selectivity) μM, respectively. Whereas QXs with glycine site K_bs of 1−18 μM had demonstrable selectivity indices ranging between 50- and only ~5-fold.

Discussion

General Overview. As a result of previous studies, QXs are commonly classed either as selective non-NMDA receptor antagonists[20] or as moderately potent NMDA receptor glycine site antagonists with low levels of selectivity versus non-NMDA receptors.[21] All the QXs in the present study were found to inhibit both types of receptors. Unexpectedly, nearly all showed steady-state selectivity indices in favor of glycine sites, and moreover, a number of trisubstituted compounds were found to be potent and highly selective glycine site ligands (Figure 2, upper panel).

Notwithstanding clear exceptions (see below), increasing potency at glycine sites generally correlates with increases in potency at non-NMDA receptors (Figure 2, middle panel). There is, however, a >10-fold greater range in the glycine site affinities; K_b values at glycine sites vary from 0.006 to 17.5 μM, whereas those at non-NMDA receptors vary between 0.47 and 100 μM. One consequence is that increases in affinity at glycine sites are not associated with parallel increases in affinity at non-NMDA receptors, and high potency at glycine sites correlates with high selectivity (Figure 2, lower panel).

Structure−Activity Relationships at the NMDA Receptor Glycine Site. The relationship between structure and activity of QXs at NMDA receptor glycine sites is summarized in Table 2. Favorable substitution patterns are able to improve potency at the NMDA receptor by as much as several thousand fold over the unsubstituted QX **6**. The most active antagonists (K_b = 5.9−7.7 nM) possess a nitro group at the 5 position and either Br or Cl, or combinations thereof, at the 6 and 7 positions. The activity of compounds **17a,b**, **24a**,

Table 2. Apparent Binding Constants of Substituted 1,4-Dihydroquinoxaline-2,3-diones to NMDA Receptor Glycine Sites and Non-NMDA Receptor Glutamate sites as Determined in Electrophysiological Assays in *Xenopus* Oocytes

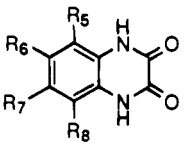

compd no.	R_5	R_6	R_7	R_8	K_b (μM) (95% confidence limits) NMDA receptor glycine site	K_b (μM) (95% confidence limits) non-NMDA receptor	selectivity for glycine site
17a	NO_2	Cl	Cl	H	0.0059 (0.0058–0.0060)	1.5 (1.4–1.6)	254
17b	NO_2	Br	Br	H	0.0065 (0.0060–0.0069)	0.89 (0.80–1.0)	140
27	NO_2	Cl	Br	H	0.0075 (0.0068–0.0084)	1.24 (1.04–1.49)	170
24a	NO_2	Br	Cl	H	0.0077 (0.0065–0.0092)	0.95 (0.85–1.07)	120
17f	NO_2	Br	CF_3	H	0.027 (0.022–0.034)	0.47 (0.45–0.49)	17
17g	NO_2	Cl	CF_3	H	0.037 (0.028–0.050)	0.55 (0.52–0.59)	15
24c	NO_2	F	Br	H	0.04 (0.035–0.046)	1.4 (1.23–1.59)	35
18x	NO_2	NO_2	Cl	H	0.042 (0.025–0.071)	0.99 (0.90–1.09)	24
18b	NH_2	Br	Br	H	0.05 (0.04–0.06)	3.32 (2.94–3.75)	66
18a	NH_2	Cl	Cl	H	0.059 (0.050–0.070)	5.19 (4.74–5.68)	88
24d	NO_2	F	Cl	H	0.019 (0.017–0.023)	1.61 (1.46–1.79)	81
10d	Cl	Cl	Cl	H	0.082 (0.070–0.096)	4.19 (3.69–4.75)	51
10i	Br	Cl	Cl	H	0.095 (0.085–0.106)	4.11 (3.37–5.01)	43
24b	NO_2	Br	F	H	0.10 (0.086–0.12)	3.45 (3.22–3.70)	35
26a	Cl	Cl	CF_3	H	0.19 (0.14–0.24)	1.23 (1.07–1.42)	6.5
26b	CF_3	Cl	Cl	H	0.19 (0.16–0.21)	2.66 (2.15–3.29)	14
10b	H	Br	Br	H	0.21 (0.17–0.26)	4.05 (3.67–4.46)	19
17c′	Cl	NO_2	CF_3	H	0.22 (0.17–0.29)	0.47 (0.45–0.53)	2.1
19	NHAc	Cl	Cl	H	0.24 (0.15–0.41)	5.57 (4.89–6.35)	23
10l	CF_3	H	Br	H	0.24 (0.20–0.29)	3.40 (2.95–3.91)	14
10f	H	Br	CF_3	H	0.26 (0.19–0.37)	1.49 (1.27–1.75)	5.7
10g	H	Cl	CF3	H	0.26 (0.22–0.37)	2.55 (2.43–2.67)	9.8
17e	NO_2	F	Cl	H	0.28 (0.24–0.33)	6.56 (5.31–8.10)	23
17x	H	Cl	NO_2	H	0.28 (0.21–0.36)	0.64 (0.46–0.88)	2.3
17h	NO_2	F	F	H	0.31 (0.29–0.33)	6.01 (5.70–6.35)	19
16a	NO_2	H	CF_3	H	0.33 (0.31–0.35)	4.13 (3.74–4.56)	13
10z	H	Br	Cl	H	0.36 (0.32–0.40)	5.70 (4.98–6.53)	16
10a	H	Cl	Cl	H	0.38 (0.34–0.43)	4.81 (4.44–5.20)	13
10m	CF_3	H	CF_3	H	0.45 (0.31–0.64)	2.21 (2.06–2.36)	4.9
16b	NO_2	Cl	H	H	0.49 (0.46–0.53)	36.4 (30.2–43.9)	74
10t	NO_2	H	Cl	H	0.51 (0.40–0.66)	8.02 (7.01–9.17)	16
10c	Cl	H	CF_3	H	0.52 (0.46–0.58)	3.70 (3.29–4.16)	7.1
10n	CF_3	H	Cl	H	0.61 (0.51–0.72)	4.67 (4.38–4.97)	7.6
10p	Cl	H	Cl	H	0.73 (0.67–0.80)	9.27 (7.93–10.8)	13
10j	Br	H	Br	H	0.89 (0.74–1.06)	6.01 (5.57–6.48)	6.8
10k	Br	H	CF_3	H	1.02 (0.84–1.23)	4.29 (3.67–5.01)	4.2
17d	NO_2	Cl	Cl	Cl	1.31 (0.98–1.74)	14.1 (11.4–17.5)	11
16c	NO_2	Br	H	H	1.32 (1.27–1.37)	36.3 (32.8–40.2)	28
10w	Cl	F	F	H	1.79 (1.61–1.99)	17.9 (14.6–21.9)	10
10e	F	Cl	F	H	1.81 (1.58–2.08)	13.2 (12.0–14.6)	7.3
10y	H	Br	H	H	2.37 (1.90–2.94)	11.22 (9.83–12.81)	4.7
17i	H	NO_2	H	H	2.40 (2.02–2.86)	1.67 (1.52–1.82)	0.7
10u	H	Cl	F	H	2.42 (2.20–2.67)	10.8 (9.36–12.5)	4.5
10s	H	F	CF_3	H	2.53 (2.21–2.89)	3.78 (3.32–4.29)	1.5
10x	H	Cl	H	H	2.62 (1.98–3.48)	16.4 (14.3–18.8)	6.3
10q	F	F	F	F	3.33 (2.92–3.81)	26.6 (23.3–30.4)	8
10o	CF_3	H	F	H	3.39 (3.02–3.80)	16.3 (15.1–17.6)	4.8
10h	H	F	F	H	4.82 (4.26–5.45)	21.5 (20.2–22.8)	4.5
10r	F	F	F	H	5.53 (4.71–6.50)	30.4 (26.5–34.9)	5.4
6	H	H	H	H	16.5 (14.7–18.5)	98.2 (75.3–128)	5.9
10v	NO_2	H	H	H	17.3 (15.8–18.9)	>100	>5.8
18c	Cl	H	CF_3	NH_2	>30	63.4 (55.4–72.5)	
17c	Cl	H	CF_3	NO_2	>30	>30	

and **27** is due to a favorable combination of all three substituents, which can be seen by analyzing compounds with only two of the three necessary substituents. Compounds **10a,b** lack the 5-nitro functionality and are about 100-fold less potent than **17a,b**. Compounds **10t** and **16b** lack one of the chlorines at the 6 or 7 position and are at least 100-fold less potent than **17a**. A drastic decrease is also seen when both halogens are removed, leaving 1,4-dihydro-5-nitroquinoxaline-2,3-dione (**10v**). The potency of this QX is roughly equal to that of the unsubstituted molecule **6**.

Other 5,6,7-trisubstituted compounds with variations of the pattern characterizing the most active structures also proved to be potent antagonists. If either the Br or Cl at the 7 position is replaced by a trifluoromethyl group, then the resulting compounds (**17f,g**) are about one-fourth to one-fifth as active as the most active antagonists. Similarly, **24b** with Br at the 6 position and F at the 7 position is only 10-fold less active than **17b** or **24a**.

Interestingly, manipulation of substituents at the 6 position reduced potency less than changes at the 7

position. Exchange of the 6-Br substituent of **17b** by a F atom results in **24c** which is about 6 times less potent than **17b** but 2.5 times more active than its 6-bromo-7-fluoro isomer **24b**. This comparison indicates that the 6 position is somewhat more tolerant toward variation than the 7 position.

Further exploration of the structural requirements at the 5 position reveals that 5-amino QXs **18a,b** are only 10-fold less active than the corresponding 5-nitro analogues **17a,b**, indicating that a powerful electron-withdrawing substituent at the 5 position is not requisite for high affinity. **19**, which is an acetyl derivative of **18a**, is 5 times less active than **18a**, indicating that a steric effect may also be operative at the 5 position. In compounds **10i,d**, the 5-nitro group of **17a** has been replaced by Br and Cl atoms, respectively. These compounds are 15-fold less active than **17a**. Other 5,6,7-trisubstituted compounds with greater deviations from the substitution pattern of **17a** are less active. In addition, replacement of a Cl or Br substituent by F invariably results in a decrease in potency. Thus, **17h** is the least active of the 5-nitro-6,7-dihalo combinations tested, while the 5,6,7-trifluorinated ligand **10r** is the least active of all the 5,6,7-trisubstituted QXs tested.

The addition of a fourth substituent decreases activity in most cases. For example, **17d** is about 200 times less potent than **17a**. Only a F atom at the 8 position is tolerated, although H is preferred. The 8-fluorinated ligand **17e** is about 4 times less active than **24d**. Tetrafluorinated QX **10q** has a higher affinity than the trifluoro analogue **10r**, although both ligands are among the least active compounds tested. Thus, substituents other than F at the 5 and/or 8 position strongly diminish affinity.

Among the disubstituted compounds, 6,7-disubstituted QXs are generally more active than 5,7-disubstituted QXs. Similar to what is observed among the trisubstituted compounds, the presence of Br, Cl, trifluoromethyl, and nitro functionalities translates into higher affinity while replacement with F decreases the affinity. The monosubstituted ligands **10x,y,v** and **17i** are particularly weak ligands at the glycine site.

Selectivity: NMDA Receptor Glycine Sites versus NMDA Glutamate Sites. The QXs assayed in this study show selectivity indices in favor of NMDA receptor glycine sites over NMDA glutamate sites. For the higher potency ligands, selectivity is at least 200-fold. Our results suggest that inhibition of NMDA receptors by QXs is dominated by interactions at glycine sites. It is unlikely that effects of these molecules *in vivo* are, to any significant extent, due to inhibition of NMDA receptors by conventional competitive antagonism at glutamate-binding sites.

Selectivity: NMDA Glycine Sites versus Non-NMDA Glutamate Receptors. The potency of 5-nitro-6-chloro QX (**16b**) and 5-nitro-6-bromo QX (**16c**) at non-NMDA receptors is atypically low when compared to other compounds with similar potency at glycine sites (Figure 2). Selectivity indices for these compounds are 74 and 28, i.e., 3–5-fold higher than would be expected for compounds with equivalent glycine site potencies. This suggests that the 5-nitro-6-chloro and, to a somewhat lesser extent, 5-nitro-6-bromo substitution patterns are unfavorable at non-NMDA sites but are well tolerated at glycine sites. One reason may be that non-NMDA sites prefer planarity of substituents in the region of the 5-nitro group. Since the 5-nitro group is twisted out of the plane of the ring (as indicated by X-ray studies of **17a,c',n**) owing to steric interaction (see supporting information), this phenomenon may contribute to the high selectivity of **17a,b**, **27**, and **24a**. It would also appear to be operating with the 5-amino-6,7-dihalogen substitution patterns (selectivity indices are 88 for **18a** and 66 for **18b**).

Conversely, potency at non-NMDA receptors is strongly favored by nitro substitutions at positions 6 and 7. Data for DNQX and CNQX have been included to help illustrate this point (Figure 2). Of the compounds tested in the present study, only the 6-nitro QX (**17i**) showed steady-state selectivity in favor of non-NMDA receptors. 5-Chloro-6-nitro-7-trifluoromethyl QX (**17c'**) and 6-chloro-7-nitro QX (**17x**) were essentially nonselective. All molecules with a nitro group at position 6 or 7 showed distinctly higher potencies at non-NMDA receptors than might be predicted from their corresponding glycine site affinity.

Potency at non-NMDA receptors also tended to be favored by a CF_3 group at position 6 or 7. For example, QXs **17f,g**, **26a**, and **10f,m,k,s** all have a 7-trifluoromethyl group, and all showed ~3–5-fold lower selectivity indices than the general trend (Figure 2, lower panel). Exceptions are **16a**, which has the glycine site-favoring 5-nitro substitution, and to a lesser extent **10g,d**, the 6-trifluoromethyl-7-chloro- and 5-chloro-7-trifluoromethyl-substituted molecules.

Our study suggests that the initial characterization of DNQX and CNQX has given a distorted impression as to the relative potencies of substituted QXs at NMDA and non-NMDA receptors.[20] The present results indicate that the selective actions of DNQX and CNQX at non-NMDA receptors are, in fact, quite atypical for this class of molecule. Most substitution patterns favor antagonism at NMDA receptors.

Selectivity indices in the present study were measured under steady-state conditions. Kinetic considerations and disparities in agonist concentrations will almost certainly affect levels of true "functional selectivity" at excitatory synapses. Indeed, previous studies characterizing the synaptic pharmacology of QXs in hippocampal slices indicate a ~6-fold reduction in functional selectivity compared to values predicted by steady-state measurements.[34] If similar factors are operating *in vivo*, then any compound with selectivity <20-fold would be rendered essentially "nonselective," and even compounds showing 100–250-fold selectivity for glycine sites would show more moderate levels of functional selectivity.

Concluding Remarks

The purpose of the present study was to identify molecules with therapeutic potential as neuroprotectants. A variety of NMDA receptor antagonists have neuroprotective actions in animal models of ischemic stroke.[8] More recently, the selective non-NMDA receptor antagonist 2,3-dihydroxy-6-nitro-7-sulfamoylbenzo[*f*]quinoxaline (NBQX) has also been shown to have neuroprotective actions *in vivo*.[37,38] The QXs **17ab**, **24a**, and **27** herein described are antagonists with nanomolar affinities at NMDA receptor glycine sites and low micromolar affinities for AMPA-preferring non-NMDA

receptors. Requirements for high potency at NMDA receptor glycine sites include the presence of a nitro group at the 5 position and either Br or Cl at the 6 and 7 positions. Other 5,6,7-trisubstituted QXs are also potent ligands, while disubstituted, monosubstituted, and tetrasubstituted QXs are less active. The four most potent compounds are also the most selective at the glycine site with respect to non-NMDA receptors. QXs **17a,b** have robust neuroprotective effects in rat models of focal ischemia.[39] We believe that this is predominantly due to inhibition at NMDA receptors, though additional inhibition at non-NMDA receptors may also play a role. Our experiments suggest that any contribution of non-NMDA receptor inhibition will be more pronounced for the moderate potency glycine site ligands such as **10d** (ACEA 1011) which is also active as a neuroprotectant in rat focal ischemia.[40]

Experimental Section

Chemistry. Melting points were taken on a Mel-Temp apparatus and are uncorrected. The samples of QXs were placed in a block preheated to 250 °C in order to minimize decomposition. ^{1}H NMR spectra were recorded at 300 MHz. Starting materials **6**, **7e–g**,l–**n**,**r**,**u**, **8a**,**h**,**j**,**p**,t, **9r**,**v**,**w**, **11a–c**, and **20a–d** were purchased from Aldrich Co., while **7b–d**,**k**,**o**,**s** and **8**t were purchased from Lancaster Co. **8d**,**i** were prepared from **8a** by adapting the method of Mitchell.[29] **8q** was prepared from pentafluoronitrobenzene using the method of Brooke.[41] ^{1}H NMR spectra of synthetic intermediates were consistent with the assigned structures. For complete characterization of QXs, refer to Table 1. The intermediate compounds were used without purification unless otherwise noted. Microanalyses were performed by Desert Analytics, Tucson, AZ. Mass spectra were recorded on a VG ZAB-2-HF mass spectrometer with a VG-11-250 data system, in the electron ionization mode (70 eV). Reverse phase HPLC were obtained at 254 nm on a 4.6 × 250 mm Microsorb-MV C18 column, using as solvents 0.1% trifluoroacetic acid in H_2O (A) and 0.1% trifluoroacetic acid in acetonitrile (B). The linear gradient was 20% B in A to 95% B in A with a flow rate of 1 mL/min. Reagents were used as received, except for *N,N*-dimethylformamide (DMF), which was dried over molecular sieves, and triethylamine and acetyl chloride, which were distilled prior to use. Aqueous $(NH_4)_2S$ (20%) (Aldrich) was diluted before use. The following general procedures are illustrative.

General Procedure A for the Nitration of Substituted Anilines: Synthesis of 4-Chloro-6-(trifluoromethyl)-2-nitroaniline (8n). A solution of 2-amino-4-chlorobenzotrifluoride (**7n**; 1.01 g, 5.16 mmol) in acetic acid anhydride (5.0 mL) was stirred at 25 °C for 12 h. The resulting suspension was filtered *in vacuo* to give 1.12 g (92%) of 4-chloro-2-(trifluoromethyl)acetanilide as white needles: mp 142–143 °C; ^{1}H NMR ($CDCl_3$) δ 7.35 (br s, 1H), 7.52 (d, 1H, J = 9.0 Hz), 7.59 (s, 1H), 8.18 (d, 1H, J = 8.1 Hz).

To a stirred solution of acetanilide (0.89 g, 3.7 mmol) dissolved in concentrated H_2SO_4 (4.0 mL) at 0 °C, concentrated HNO_3 (0.5 mL) was added dropwise. The resulting solution was allowed to warm to room temperature and stirred at room temperature for 3 h. It was then poured into ice water (15 mL). The resulting suspension was filtered *in vacuo* to give 0.700 g of crude product which was crystallized from EtOH–H_2O to give 0.560 g (53%) of 4-chloro-6-(trifluoromethyl)-2-nitroacetanilide as yellow needles: mp 186–188 °C; ^{1}H NMR ($CDCl_3$) δ 7.37 (s, 1H), 7.90 (d, 1H, J = 2.1 Hz), 8.11 (d, 1H, J = 2.1 Hz).

A solution of 2-nitroacetanilide (0.35 g, 1.2 mmol) and concentrated HCl (3.0 mL) was refluxed overnight. The mixture was extracted with EtOAc (2 × 3.0 mL). The ethyl acetate extract was washed with brine, dried, and concentrated *in vacuo* to give 0.25 g (40% overall yield) of **8n** as a shining yellow powder: mp 65–69 °C; ^{1}H NMR δ 6.65 (br s, 2H), 7.72 (d, 1H, J = 2.1 Hz), 8.36 (d, 1H, J = 2.1 Hz).

General Procedure B for the Nitration of Substituted Anilines: Synthesis of 3-Chloro-2,4-difluoro-6-nitroaniline (8e). To a stirred solution of 3-chloro-2,4-difluoroaniline (10.5 g, 64.3 mmol) in dioxane (25 mL) in an ice bath was added dropwise trifluoroacetic anhydride (14.8 g, 70.4 mmol). The solution was warmed to room temperature and stirred at room temperature for 20 h. The solution was then poured into ice–water (150 mL) and stirred for 1 h. The resulting suspension was filtered *in vacuo*, washed with water (50 mL), and dried to give 16.1 g (96%) of 3-chloro-2,4-difluoro-1-(trifluoroacetamido)benzene as an almost colorless powder: mp 73–74 °C; ^{1}H NMR ($CDCl_3$) δ 7.07 (m, 1H), 7.98 (br s, 1H), 8.15 (m, 1H).

To a stirred solution of 3-chloro-2,4-difluoro-1-(trifluoroacetamido)benzene (15.1 g, 58.1 mmol) in concentrated H_2SO_4 (80 mL) in an ice bath was added dropwise concentrated HNO_3 (10 mL). The resulting suspension was stirred in an ice bath for 4 h and poured into ice–water (600 mL). The resulting suspension was filtered *in vacuo* and washed with water (100 mL) to give 16.8 g (95%) of 3-chloro-2,4-difluoro-1-(trifluoroacetamido)-6-nitrobenzene as an almost colorless powder: mp 124–125 °C; ^{1}H NMR ($CDCl_3$) δ 7.69 (dd, 1H, J = 1.6, 8.0 Hz), 8.94 (br s, 1H).

A solution of 3-chloro-2,4-difluoro-1-(trifluoroacetamido)-6-nitrobenzene (6.35 g, 20.8 mmol) in MeOH/7% aqueous K_2CO_3 (3:2, 60 mL) was stirred at room temperature for 4 h. The resulting suspension was filtered *in vacuo*, washed with water, and dried to give 0.301 g of **8e** as a yellow powder: mp 96–97 °C; ^{1}H NMR ($CDCl_3$) δ 6.07 (br s, 2H), 7.82 (dd, 1H, J = 1.9, 9.0 Hz); 3.5 g of additional **8e** was isolated from the filtrate to give a total yield of 3.8 g (87%).

General Procedure C for the Nitration of Substituted Anilines: Synthesis of 2,3,4-Trifluoro-6-nitroaniline (8r). To a pink solution of 2,3,4-trifluoroaniline (**7s**; 1.04 g, 9.45 mmol) in $CHCl_3$ (12 mL) was added acetic anhydride (1.63 g, 16.0 mmol), giving a pale purple solution which was stirred overnight under nitrogen. The solvent was removed *in vacuo*, and the resulting solid was then allowed to air-dry to give 1.35 g (99%) of 2,3,4-trifluoroacetanilide as a white powder: mp 98–100 °C; ^{1}H NMR ($CDCl_3$) δ 6.91–7.00 (m, 1H), 7.22 (br s, 1H), 7.96–8.04 (m, 1H).

The nitration was accomplished adapting the procedure of Cheeseman.[23] To a stirred solution of the 2,3,4-trifluoroacetanilide (0.526 g, 2.78 mmol) in concentrated H_2SO_4 (3 mL) in an ice bath was slowly added KNO_3 (0.281 g, 2.78 mmol). The resulting pale brown solution was stirred overnight at room temperature. The dark red solution was carefully neutralized by adding saturated $NaHCO_3$ solution. The red solution was extracted with CH_2Cl_2 (4 × 20 mL). The CH_2Cl_2 extract was dried over anhydrous Na_2SO_4 and removed *in vacuo* to give 0.333 g of an amber powder which was purified on silica gel using hexane–chloroform (1:1) as eluant to give 0.258 g (48%) of **8r** as a crystalline golden solid: mp 56–58 °C; ^{1}H NMR ($CDCl_3$) δ 6.12 (br s, 2H), 7.32 (dd, 1H, J = 6.0, 9.2 Hz).

General Procedure D for the Reduction of Substituted 2-Nitroanilines to Substituted 1,2-Diaminobenzenes: Synthesis of 1,2-Diamino-3-bromo-4,5-dichlorobenzene (9i). The procedure of Bellamy and Ou[25] was adapted as follows. A suspension of 2-bromo-3,4-dichloro-6-nitroaniline (**8i**; 0.35 g, 1.2 mmol) and $SnCl_2 \cdot H_2O$ (1.90 g, 6.5 mmol) in EtOAc (3.7 mL) and EtOH (1.9 mL) was stirred at 70 °C for 35 min. The resulting brown solution was added to crushed ice (12 mL) and carefully neutralized using aqueous $NaHCO_3$. The resulting suspension was extracted with EtOAc (3 × 15 mL). The combined EtOAc extract was washed with brine, dried, and removed *in vacuo* to give 0.26 g (84%) of **9i** as a brown powder: mp 123–125 °C; ^{1}H NMR ($CDCl_3$) δ 3.49 (br s, 2H), 3.96 (br s, 2H), 6.80 (s, 1H).

General Procedure E for the Reduction of Substituted 2-Nitroanilines to Substituted 1,2-Diaminobenzenes: Synthesis of 1,2-Diamino-4-chloro-3,5-difluorobenzene (9e). To a solution of 3-chloro-2,4-difluoro-6-nitroaniline (**8e**; 3.60 g, 17.3 mmol) in CH_3OH (25 mL) was added 10% Pd/C (0.20 g). The mixture was hydrogenated at 20–30 psi for 3 h. The catalyst was filtered, and the filtrate was evaporated to

dryness. The residual solid was crystallized from hexane to give 2.97 g (96%) of diamine **9e** as brown needles: mp 77–78 °C; ^{1}H NMR ($CDCl_3$) δ 3.16 (br s, 2H), 3.70 (br s, 2H), 6.35 (dd, 1H , J = 1.8, 9.9 Hz).

General Procedure F for the Selective Reduction of Substituted 2,6-Dinitroanilines to Substituted 1,2-Diamino-3-nitrobenzenes: Synthesis of 1,2-Diamino-5-chloro-3-nitrobenzene (9t). The procedure of Gillespie et al.[26] was adapted as follows. A suspension of **8t** (0.26 g, 1.2 mmol) in 6.7% aqueous $(NH_4)_2S$ (8.0 mL) and EtOH (8.0 mL) was refluxed for 45 min. The resulting dark red solution was cooled to room temperature, and the solid was collected by filtration *in vacuo* to give 0.181 g (80%) of diamine **9t** as shiny red needles: mp 161–163 °C dec; ^{1}H NMR ($CDCl_3$) δ 5.03 (br s, 1H), 6.69 (br s, 1H), 6.91 (d, 1H, J = 2.4 Hz), 7.41 (d, 1H, J = 2.4 Hz).

General Procedure G for the Conversion of Substituted 1,2-Diaminobenzenes to Substituted QXs: Synthesis of 5,7-Dibromo QX (10j). The procedure of Cheeseman[23] was adapted as follows. A solution of diethyl oxalate (2.19 g, 15.0 mmol) and **9j** (0.40 g, 1.5 mmol) was heated to reflux under N_2 for 6 h. The resulting suspension was cooled to room temperature, and the solid was collected by vacuum filtration, washed with EtOH, and dried in air to give 0.260 g (55%) of crude **10j**. A portion of this solid (0.150 g) was dissolved in 1 N aqueous NaOH (20 mL) by gently heating on a steam bath. The solution was treated with activated charcoal and filtered. The pH of the filtrate was adjusted with 1 N HCl to 1. The yellow suspension was filtered *in vacuo*, washed with water (20 mL), and dried *in vacuo* to give 0.050 g (18%) of **10j** as yellow needles (Table 1).

General Procedure H for the Conversion of Substituted 1,2-Diaminobenzenes to Substituted QXs: Synthesis of 6,7-Dichloro QX (10a). The procedure of Foged et al.[24] was adapted as follows. A suspension of 4,5-dichloro-*o*-phenylenediamine (2.65 g, 15.0 mmol) and oxalic acid dihydrate (1.986 g, 15.75 mmol) in 2 N aqueous HCl (22.5 mL) was refluxed for 2.5 h. The resulting suspension was cooled to room temperature and diluted with water (50 mL). The solid was collected by vacuum filtration, washed with water (150 mL), and dried at *in vacuo* at 60 °C to give 3.39 g (98%) of **10a** as a deep pink powder (Table 1).

General Procedure I for the Conversion of Substituted 2-Nitroanilines to Substituted QXs via Selenium Heterocycles: Synthesis of 6-Chloro-1,4-dihydro-5-nitroquinoxaline-2,3-dione (16b). Using method D, **11b** was converted to diamine **12b**. To a refluxing solution of **12b** (0.643 g, 4.51 mmol) in ethanol (5 mL) was added dropwise a solution of SeO_2 (0.550 g, 4.95 mmol) in water (2.3 mL). The resulting suspension was refluxed for 30 min and cooled to room temperature. The solid was collected by vacuum filtration, washed with water (5 mL), and dried *in vacuo* to give 0.801 g (81%) of 5-chloro-2,1,3-benzoselenadiazole (**13b**) as a light brown powder: mp 116–117 °C (lit.[42] mp 118–119 °C); ^{1}H NMR (DMSO-d_6) δ 7.53 (dd, 1H, J = 2.1, 9.6 Hz), 7.84 (d, 1H, J = 9.6 Hz), 7.98 (d, 1H, J = 1.8 Hz).

To a stirred, dark red solution of **13b** (0.200 g, 0.919 mmol) in concentrated H_2SO_4 (3 mL) at 10 °C was added concentrated HNO_3 (0.20 mL, 3.0 mmol), and the resulting yellow solution was stirred at 10 °C for 1 h. It was then poured into ice–water (30 mL), and the solid was collected by vacuum filtration, washed with water (10 mL), and dried *in vacuo* to give 0.219 g (90%) of 5-chloro-4-nitro-2,1,3-benzoselenadiazole (**14b**) as a yellow powder: mp 228–230 °C (lit.[28a] mp 230–232 °C); ^{1}H NMR (DMSO-d_6) δ 7.82 (d, 1H, J = 9.6 Hz), 8.13 (d, 1H, J = 9.6 Hz).

To a stirred suspension of **14b** (0.160 g, 0.610 mmol) in concentrated HCl (1.5 mL) was added, 48% HI (0.5 mL) and the mixture was stirred at room temperature for 2 h. Aqueous $NaHSO_3$ (5%) (3 mL) was added to react with the liberated I_2. The pH was adjusted with 50% NaOH to 8 and the mixture extracted with EtOAc (2 × 20 mL). The EtOAc extract was washed with brine, dried, and removed *in vacuo* to give 0.101 g (88%) of 4-chloro-3-nitro-1,2-phenylenediamine (**15b**) as a red powder: mp 124–126 °C (lit.[28b] mp 127.5–129.5 °C); ^{1}H NMR (acetone-d_6) δ 4.78 (br s, 2H), 5.12 (br s, 2H), 6.64 (d, 1H, J = 8.4 Hz), 6.76 (d, 1H, J = 8.4 Hz).

Method H was used to convert **15b** to quinoxalinedione **16b**.

General Procedure J for the Nitration of QXs: Synthesis of 6,7-Dichloro-1,4-dihydro-5-nitroquinoxaline-2,3-dione (17a). The procedure of Cheeseman[23] was adapted as follows. To a stirred solution of **10a** (3.33 g, 14.5 mmol) in concentrated H_2SO_4 (65 mL) in an ice bath was added KNO_3 (2.20 g, 21.8 mmol) in portions over 10 min. The resulting solution was stirred at room temperature for 20 h and slowly poured into ice–water (400 mL). The solid was collected by vacuum filtration, washed with water (50 mL), and dried *in vacuo* to give 3.39 g (85%) of **17a** as a yellow powder. It was purified as follows. **17a** (3.365 g) was added to 1 N aqueous NaOH (550 mL) and stirred vigorously for 20 min. The resulting suspension was filtered *in vacuo* to remove a small amount of insoluble material. The pH of the filtrate was adjusted from 13 to 11 by dropwise addition of concentrated HCl (43 mL) and monitoring by pH meter. The solid was collected by vacuum filtration and washed with water (250 mL). The moist product was taken up as a suspension in water (200 mL), and concentrated HCl was added dropwise to adjust the pH to 5. After stirring at pH 5 for 30 min, the solid was collected by vacuum filtration, washed with water (400 mL), and dried *in vacuo* at 60 °C to give 3.12 g (93%) of **17a** as a yellow powder (Table 1).

General Procedure K for the Nitration of QXs: Synthesis of 6,7-Difluoro-1,4-dihydro-5-nitroquinoxaline-2,3-dione (17h). To a stirred suspension of **10h** (0.837 g, 4.23 mmol) in TFA (30 mL) was added KNO_3 (0.512 g, 5.07 mmol). The mixture was stirred at 55 °C for 20 h. KNO_3 (0.256 g, 2.53 mmol) was added to the mixture and the mixture stirred further at 55 °C for 20 h. A final addition of KNO_3 (0.256 g, 2.53 mmol) was made, and the mixture was again stirred for 20 h at 55 °C. The reaction mixture was concentrated *in vacuo*, and the residual paste was added to cold H_2O. The solid was collected by vacuum filtration, washed with cold H_2O (25 mL), and dried *in vacuo* to give 0.700 g (68%) of **17h** as a yellow powder (Table 1).

General Procedure L for the Reduction of 1,4-Dihydro-5-nitroquinoxaline-2,3-diones to 5-Amino QXs: Synthesis of 5-Amino-6,7-dibromo QX (18b). The procedure of Bellamy and Ou[25] was adapted as follows. A solution of **17b** (0.300 g, 0.82 mmol) and $SnCl_2 \cdot 2H_2O$ (0.925 g, 4.10 mmol) in EtOH (10 mL) and DMSO (0.5 mL) was stirred at 80 °C for 2.5 h. It was then cooled to room temperature, and the solid was collected by vacuum filtration, washed with cold EtOH (4 mL), and dried to give crude **18b** which was purified by crystallization from DMSO–H_2O to give 0.160 g (59%) of **18b** as bright yellow needles (Table 1).

General Procedure M for Conversion of 5-Amino QXs to 5-Acetamido QXs: Synthesis of 5-Acetamido-6,7-dichloro QX (19). To a stirred solution of **18a** (0.062 g, 0.25 mmol) in DMF (7 mL) were added Et_3N (0.033 g, 0.33 mmol) and acetyl chloride (0.020 g, 0.26 mmol). The mixture was stirred overnight at room temperature to give a white suspension. The solid was collected by vacuum filtration and washed with H_2O (2 mL) to give crude **19** as a white solid. It was crystallized from DMSO–H_2O to yield 0.025 g (35%) of **19** as a white powder (Table 1).

General Procedure N for the Conversion of 3,4-Disubstituted Fluorobenzenes to 6,7-Disubstituted-1,4-dihydro-5-nitroquinoxaline-2,3-diones: Synthesis of 6-Bromo-7-fluoro-1,4-dihydro-5-nitroquinoxaline-2,3-dione (24b). To a stirred solution of **20b** (1.000 g, 5.181 mmol) in concentrated H_2SO_4 (8 mL) at 0 °C was added KNO_3 (0.525 g, 5.19 mmol) in one portion. The resulting yellow solution was allowed to warm to room temperature and stirred overnight at room temperature. The solution was poured into ice (80 g) and extracted with ethyl acetate (75 mL). The ethyl acetate extract was washed with water and brine, dried and concentrated. The residual solid was dried *in vacuo* to give 1.105 g (89%) of **21b** as a white powder: mp 58–60 °C; ^{1}H NMR ($CDCl_3$) δ 7.59 (dd, 1H, J = 5.4, 9.6 Hz), 7.89 (t, 1H, J = 6.9 Hz).

To a stirred solution of **21b** (1.100 g, 4.622 mmol) in DMF (11 mL) at 70 °C was added dropwise a solution of sodium glycinate (0.451 g, 4.65 mmol) in water (5 mL). The resulting solution was stirred overnight at 70 °C. The solution was then cooled to room temperature resulting in a bright orange suspension. The solid was collected by vacuum filtration, washed with $CHCl_3$ (10 mL) and dried *in vacuo* to give 0.690 g (51%) of **22b** as a bright orange powder: mp 252 °C dec; ^1H NMR (DMSO-d_6) δ 3.46 (d, 2H, J = 3.9 Hz), 7.15 (d, 1H, J = 6.0 Hz), 7.94 (d, 1H, J = 9.3 Hz), 8.74 (s, 1H).

A solution of **22b** (0.650 g, 2.22 mmol) and tin(II) chloride dihydrate (1.501 g, 6.66 mmol) in ethanol (10 mL) was refluxed for 30 min. It was then cooled to room temperature, and the solvent was removed *in vacuo*. The residual slurry was diluted with water (15 mL), and the pH was adjusted with 10% Na_2CO_3 to 8. The resulting suspension was extracted with ethyl acetate (100 mL). The ethyl acetate extract was washed with water and brine, dried, and concentrated. The residual solid was dried *in vacuo* to give 0.348 g (64%) of **23b** as a yellow powder: mp 214–216 °C dec; ^1H NMR (DMSO-d_6) δ 3.68 (s, 2H), 6.06 (s, 1H), 6.63 (d, 1H, J = 9.3 Hz), 6.83 (d, 1H, J = 6.6 Hz), 10.30 (s, 1H).

To a stirred solution of **23b** (0.050 g, 0.20 mmol) in TFA (0.5 mL) was added excess fuming HNO_3 (0.17 mL, 3.9 mmol), and the red solution was stirred overnight at room temperature. The resulting yellow suspension was poured into ice–water (3 mL). The solid was collected by vacuum filtration, washed with water (3 mL), and dried *in vacuo* to give 0.053 g (85%, 24.7% overall) of **24b** as a yellow powder (Table 1).

General Procedure O: Synthesis of 5,6-Dichloro-7-trifluoromethyl QX (26a). **17c'** was reduced to **25a** using procedure L. A mixture of **25a** (0.054 g, 0.19 mmol) in concentrated HCl (2 mL) was stirred in an ice bath for 1 h. To the mixture was added dropwise a solution of $NaNO_2$ (60 mg, 0.86 mmol) in H_2O (0.3 mL), and the resulting solution was stirred in an ice bath for 3 h. To the red solution was added a cold solution of CuCl (120 mg) in 6 N HCl (1.2 mL), and the stirring was continued in an ice bath for 2 h followed by overnight at room temperature. The resulting mixture was diluted with 1 N HCl (3 mL), stirred at room temperature for 30 min, and finally diluted with H_2O (2 mL). The solid was collected by filtration, washed with water, and dried to give 0.030 g (52%) of **26a** as a white powder (Table 1).

General Procedure P for Halogenation:[29] Synthesis of 7-Bromo-6-chloro-1,4-dihydro-5-nitroquinoxaline-2,3-dione (27). To a stirred solution of **16b** (0.035 g, 0.14 mmol) in DMF (0.5 mL) was added NBS (0.039 g, 0.22 mmol), and the solution was stirred at room temperature for for 5 days. The resulting solution was diluted with water (4 mL), and the yellow solid was collected by vacuum filtration, washed with water (2 mL), and dried *in vacuo* to give 0.042 g of crude **27** which was crystallized three times from DMSO–water to give 0.018 g (44%) of **27** as shining yellow flakes (Table 1). Similar procedure was carried out for the chlorination by substituting NBS with NCS.

Electrophysiology. Total RNA from whole rat brain (including cerebellum and a portion of the brain stem) was prepared by the acid guanidinium/phenol method.[43] Poly(A)$^+$ RNA was isolated by oligo(dT) chromatography. Following established procedures,[44] ovarian lobes were surgically removed from mature female *Xenopus laevis*, and oocytes (stages V–VI) were dissected from the ovary, microinjected with approximately 50 ng of whole rat brain poly(A)$^+$ RNA, and stored in Barth's medium containing (in mM): NaCl, 88; KCl, 1; $CaCl_2$, 0.41; $Ca(NO_3)_2$, 0.33; $MgSO_4$, 0.82; $NaHCO_3$, 2.4; HEPES, 5; pH 7.4, with 0.1 mg/mL gentamycin sulfate. Oocytes were defolliculated 1–2 days following injection by treatment (0.5–1 h) with collagenase (0.5 mg/mL, Sigma type I). Recordings were made 3–10 days following injection using a two-electrode voltage clamp (Dagan TEV-200) in a 0.1 mL recording chamber continuously perfused (5–15 mL min^{-1}) with frog Ringer's solution containing (in mM): NaCl, 115; KCl, 2; $CaCl_2$, 1.8; HEPES, 5; pH 7.4. Drugs were applied by bath perfusion, and Ringer's solution pH was readjusted to 7.4 where necessary. DNQX and CNQX were obtained from Research Biomedicals Inc. (Natick, MA). Other drugs were from Sigma. QXs were made up in DMSO. Depending upon potency of antagonism, DMSO stock concentrations varied over the range 0.3 μM–100 mM. Ringer solutions of QXs were made by 1000–3000-fold dilution of DMSO stocks into Ringer's solution. At 0.03–0.3% (by vol) DMSO alone did not appreciably affect the amplitudes of membrane current responses. Stocks were stored for up to 4 weeks in the dark at 4 °C without reduction in potency. Ringer solutions of drugs were made up fresh, minutes prior to each experiment.

Data Analysis. Concentration–response data were fit to the logistic equation (eq 1): n is the slope factor, EC_{50} is the agonist concentration that produces a half-maximal response, and pEC_{50} is $-\log EC_{50}$ (Sigmaplot, Jandel Scientific).

$$I/I_{max} = 1/(1 + (10^{-pEC_{50}}/[agonist])^n) \quad (1)$$

Partial concentration–inhibition curves were fit with eq 2:

$$I/I_{control} = 1/(1 + ([antagonist]/10^{-pIC_{50}}))^n \quad (2)$$

in which $I_{control}$ is response activated by agonist alone, IC_{50} is the concentration of antagonist that produces half-maximal inhibition, pIC_{50} is $-\log IC_{50}$, and n is the slope factor. The K_b values for antagonists were determined from inhibition curves using eq 3:

$$K_b = F(IC_{50}(2 + ([agonist]_f/EC_{50})^b)^{1/b} - 1) \quad (3)$$

a Leff–Dougall-generalized variant of the Cheng–Prusoff equation,[36] where $[agonist]_f$ is the fixed dose of agonist. In practice, the parameter $10^{-pIC_{50}}$ was replaced in eq 2 by $10^{-pK_b}((2 + ([agonist]_f/EC_{50})^b)^{1/b}) - 1)$; 95% confidence intervals for pK_b were obtained as the product of the standard deviation for each parameter multiplied by the t distribution value. Confidence intervals in Table 2 have been transformed to the linear scale. Data quoted in the text is given as mean ± SEM.

Acknowledgment. Financial support was provided by Acea Pharmaceuticals, Inc., A Subsidiary of CoCensys, Inc., and the National Institute of Drug Abuse (DA-06726). We thank Dr. Kyle Gee and Ms. H. Zheng for the synthesis of **8r** and **10i**, respectively. We also thank Dr. Timothy Weakley for the X-ray crystallographic determinations.

Supporting Information Available: Accounts of structural analysis and listings of crystallographic properties and numerical details of refinement, atomic coordinates, bond lengths and angles, anisotropic thermal parameters, contact distances, torsion angles, mean planes, and ORTEP diagrams for compounds **17a,c',n** (41 pages); tables of observed and calculated structural factors (44 pages). Ordering information is given on any current masthead page.

References

(1) (a) McCulloch, J. Excitatory Amino Acid Antagonists and their Potential for the Treatment of Ischeamic Brain Damage in Man. *Br. J. Clin. Pharmacol.* **1992**, *34*, 106–114. (b) Dodd, P. R.; Scott, H. L.; Westphalen, R. I. Excitatoxic Mechanisms in the Pathogenesis of Dementia. *Neurochem. Int.* **1994**, *25*, 203–219. (c) Lipton, S. A. Models of Neuronal Injury in AIDS: Another Role for the NMDA Receptor? *Trends Neurosci.* **1992**, *15*, 75–79.

(2) (a) Choi, D. W.; Rothman, S. M. The Role of Glutamate Neurotoxicity in Hypoxic-Ischemic Neuronal Death. *Annu. Rev. Neurosci.* **1990**, *13*, 171–182. (b) Meldrum, B.; Garthwaite, J. Excitatory Amino Acid Neurotoxicity and Neurodegenerative Disease. *Trends Pharmacol. Sci.* **1990**, *11*, 379–387.

(3) Wong, E. H. F.; Kemp, J. A. Sites for Antagonism on the *N*-Methyl-D-aspartate Receptor Channel Complex. *Annu. Rev. Pharmacol. Toxicol.* **1991**, *31*, 401–425.

(4) (a) Wong, E. H. F.; Kemp, J. A.; Priestley, T.; Knight, A. R.; Woodruff, G. N.; Iversen, L. L. The Anticonvulsant MK-801 is a Potent *N*-Methyl-D-aspartate Antagonist. *Proc. Natl. Acad. Sci. U.S.A.* **1986**, *83*, 7104–7108. (b) Huettner, J. E.; Bean, B. P. Block of *N*-Methyl-D-aspartate-activated Current by the Anticonvulsant MK-801: Selective Binding to Open Channels. *Proc. Natl. Acad. Sci. U.S.A.* **1988**, *85*, 1307–1311.

(5) (a) Foster, A. C.; Fagg, G. E. Acidic Amino Acid Binding Sites in Mammalian Neuronal Membranes: Their Characteristics and Relationship to Synaptic Receptors. *Brain Res.* **1984**, *319*, 103–164. (b) Watkins, J. C.; Olverman, H. J. Agonists and Antagonists for Excitatory Amino Acid Receptors. *Trends Neurosci.* **1987**, *10*, 265–272.

(6) (a) Johnson, J. W.; Ascher, P. Glycine Potentiates the NMDA Response in Cultured Mouse Brain Neurons. *Nature (London)* **1987**, *325*, 529–531. (b) Kleckner, N. W.; Dingledine, R. Requirement for Glycine in Activation of NMDA Receptors Expressed in Xenopus Oocytes. *Science (Washington, D.C.)* **1988**, *241*, 835–837.

(7) Williams, K.; Romano, C.; Dichter, M. A.; Molinoff, P. B. Minireview: Modulation of the NMDA Receptor by Polyamines. *Life Sci.* **1991**, *48*, 469–498.

(8) (a) Park, C. K.; Nehls, D. G.; Graham, D. I.; Teasdale, G. M.; McCulloch, J. Focal Cerebral Ischemia in the Cat: Treatment with the Glutamate Antagonist MK-801 after Induction of Ischemia. *J. Cereb. Blood Flow Metab.* **1988**, *8*, 757–762. (b) Boast, C. A.; Gerhardt, S. C.; Pastor, G.; Lehmann, J.; Etienne, P. E.; Liebman, J. M. The *N*-Methyl-D-aspartate Antagonists cgs 19755 and CPP Reduce Ischemic Brain Damage in Gerbils. *Brain Res.* **1988**, *442*, 345–348. (c) Schoepp, D. D.; Ornstein, P. L.; Salhoff, C. R.; Leander, J. D. Neuroprotectant Effects of LY 274614, a Structurally Novel Systemically Active Competitive NMDA Receptor Antagonist. *J. Neural Transm. (Gen. Sect.)* **1991**, *85*, 131–143.

(9) (a) Tricklebank, M. D.; Singh, L.; Oles, R. J.; Preston, C.; Iverson, S. D. The Behavioral Effects of MK-801: A Comparison with Antagonists Acting Noncompetitively and Competitively at the NMDA Receptor. *Eur. J. Pharmacol.* **1989**, *167*, 127–135. (b) Willetts, J.; Balster, R. L.; Leander, J. D. The Behavioral Pharmacology of NMDA Receptor Antagonists. *Trends Pharmacol. Sci.* **1990**, *11*, 423–428.

(10) Koek, W.; Colpaert, F. C. *N*-Methyl-D-aspartate Antagonism and Phencyclidine-like Activity: Behavioral Effects of Glycine Site Ligands. In *Multiple Sigma and PCP Receptor Ligands: Mechanisms for Neuromodulation and Neuroprotection*; Kamenka, J.-M., Domino, E. F., Eds.; CPP Books: Ann Arbor, MI, 1992; pp 665–671.

(11) Singh, L.; Menzies, R.; Tricklebank, M. D. The Discriminative Stimulus Properties of (+)-HA-966, an Antagonist at the Glycine/*N*-Methyl-D-aspartate Receptor. *Eur. J. Pharmacol.* **1990**, *186*, 129–132.

(12) Balster, R. L.; Grech, D. M.; Mansbach, R. S.; Li, H.; Weber, E. Behavioral Studies on the Novel Glycine-site NMDA Antagonists ACEA-1011 and ACEA-1021 in Rats. *Soc. Neurosci. Abstr.* **1993**, 19,472,197.16.

(13) (a) Olney, J. W.; Labruyere, J.; Price, M. T. Pathological Changes Induced in Cerebrocortical Neurons by Phencyclidine and Related Drugs. *Science (Washington, D.C.)* **1989**, *244*, 1360–1362. (b) Hargreaves, R. J.; Rigby, M.; Smith, D.; Hill, R. G.; Iversen, L. L. Competitive as well as uncompetitive *N*-Methyl-D-aspartate Receptor Antagonists Affect Cortical Neuronal Morphology and Cerebral Glucose Metabolism. *Neurochem. Res.* **1993**, *18*, 1263–1269. (c) Hargreaves, R. J.; Rigby, M.; Smith, D.; Hill, R. G. Lack of Effect of L-687,414 ((+)-*cis*-4-Methyl-HA-966), an NMDA Receptor Antagonist Acting at the Glycine Site, on Cerebral Glucose Metabolism and Cortical Neuronal Morphology. *Br. J. Pharmacol.* **1993**, *110*, 36–42.

(14) (a) Kemp, J. A.; Leeson, P. D. The Glycine Site of the NMDA Receptor - Five Years On. *Trends Pharmacol. Sci.* **1993**, *14*, 20–25. (b) Leeson, P. D. Glycine-site *N*-Methyl-D-aspartate Receptor Antagonists. In *Drug Design for Neuroscience*; Kozikowski, A. P., Ed.; Raven Press Ltd.: New York, 1993; pp 339–381.

(15) Leeson, P. D.; Baker, R.; Carling, R. W.; Curtis, N. R.; Moore, K. W.; Williams, B. J.; Foster, A. C.; Donald, A. E.; Kemp, J. A.; Marshall, G. R. Kynurenic Acid Derivatives. Structure-Activity Relationships for Excitatory Amino Acid Antagonism and Identification of Potent and Selective Antagonists at the Glycine Site on the *N*-Methyl-D-aspartate Receptor. *J. Med. Chem.* **1991**, *34*, 1243–1252.

(16) Carling, R. W.; Leeson, P. D.; Moseley, A. M.; Baker, R.; Foster, A. C.; Grimwood, S.; Kemp, J. A.; Marshall, G. R. 2-Carboxytetrahydroquinolines. Conformational and Stereochemical Requirements for Antagonism of the Glycine Site on the NMDA Receptor. *J. Med. Chem.* **1992**, *35*, 1942–1953.

(17) Nagata, R.; Tanno, N.; Kodo, T.; Ae, N.; Yamaguchi, H.; Nishimura, T.; Antoku, F.; Tatsuno, T.; Kato, T.; Tanaka, Y.; Nakamura, M. Tricyclic Quinoxalinediones: 5,6-Dihydro-1*H*-pyrrolo[1,2,3-*de*]quinoxaline-2,3-diones and 6,7-Dihydro-1*H*,5*H*-pyrido[1,2,3-*de*]quinoxaline-2,3-diones as Potent Antagonists for the Glycine Binding Site of the NMDA Receptor. *J. Med. Chem.* **1994**, *37*, 3956–3968.

(18) Swartz, K. J.; Koroshetz, W. J.; Rees, A. H.; Huettner, J. E. Competitive Antagonism of Glutamate Receptor Channels by Substituted Benzazepines in Cultured Cortical Neurons. *Mol. Pharmacol.* **1992**, *41*, 1130–1141.

(19) (a) Kulagowski, J. J.; Baker, R.; Curtis, N. R.; Leeson, P. D.; Mawer, I. M.; Moseley, A. M.; Ridgill, M. P.; Rowley, M.; Stansfield, I.; Foster, A. C.; Grimwood, S.; Hill, R. G.; Kemp, J. A.; Marshall, G. R.; Saywell, K. L.; Tricklebank, M. D. 3′-(Arylmethyl)- and 3′-(Aryloxy)-3-phenyl-4-hydroxyquinolin-2(1*H*)-ones: Orally Active Antagonists of the Glycine Site on the NMDA Receptor. *J. Med. Chem.* **1994**, *37*, 1402–1405. (b) McQuaid, L. A.; Smith, E. C. R.; Lodge, D.; Pralong, E.; Wikel, J. H.; Calligaro, D. O.; O'Malley, P. J. 3-Phenyl-4-hydroxyquinolin-2(1*H*)-ones: Potent and Selective Antagonists at the Strychnine-insensitive Glycine Site on the *N*-Methyl-D-aspartate Receptor Complex. *J. Med. Chem.* **1992**, *35*, 3423–3425.

(20) (a) Honore, T.; Davies, S. N.; Drejer, J.; Fletcher, E. J.; Jacobsen, P.; Lodge, D.; Nielsen, F. E. Quinoxalinediones: Potent Competitive Non-NMDA Glutamate Receptor Antagonists. *Science (Washington, D.C.)* **1988**, *241*, 701–703. (b) Fletcher, E. J.; Martin, D.; Aram, J. A.; Lodge, D.; Honore, T. Quinoxalinediones Selectively Block Quisqualate and Kainate Receptors and Synaptic Events in Rat Neocortex and Hippocampus and Frog Spinal Cord *in vitro*. *Br. J. Pharmacol.* **1988**, *95*, 585–597.

(21) (a) Birch, P. J.; Grossman, C. J.; Hayes, A. G. 6,7-Dinitroquioxaline-2,3-dione and 6-Nitro-7-cyano-quinoxaline-2,3-dione Antagonize Responses to NMDA in the Rat Spinal Cord via an Action at the Strychnine-insensitive Glycine Receptor. *Eur. J. Pharmacol.* **1988**, *156*, 177–180. (b) Sheardown, M. J.; Drejer, J.; Jensen, L. H.; Stidsen, C. E.; Honore, T. A Potent Antagonist of the Strychnine-insensitive Glycine Receptor has Anticonvulsant Properties. *Eur. J. Pharmacol.* **1989**, *174*, 197–204. (c) Yoneda, Y.; Ogita, K. Abolition of the NMDA-Mediated Response by a Specific Glycine Antagonist, 6,7-Dichloroquinoxaline-2,3-dione (DCQX). *Biochem. Biophys. Res. Commun.* **1989**, *164*, 841–849. (d) Lester, R. A. J.; Quarum, M. L.; Parker, J. D.; Weber, E.; Jahr, C. E. Interaction of 6-Cyano-7-nitroquinoxaline-2,3-dione with the *N*-Methyl-D-aspartate Receptor-Associated Glycine Binding Site. *Mol. Pharmacol.* **1989**, *35*, 565–570.

(22) Cai, S. X.; Dinsmore, C. M.; Gee, K. R.; Glenn, A. G.; Huang, J. C.; Johnson, B. L.; Kher, S. M.; Lü, Y.; Oldfield, P. L.; Marek, P.; Woodward, R. M.; Zheng, H.; Weber, E.; Keana, J. F. W. Preparation of Multisubstituted Quinoxaline-2,3-diones as Antagonists for the NMDA Receptor Glycine Site. Presented at the 207th ACS National Meeting, San Diego, CA, March 1994; Division of Medicinal Chemistry Abstract 184.

(23) Cheeseman, G. W. H. Quinoxalines and Related Compounds Part VI. Substitution of 2,3-Dihydroxyquinoxaline and its 1,4-Dimethyl Derivative. *J. Chem. Soc.* **1962**, 1170–1176.

(24) Foged, C.; Jacobsen, P. Synthesis of ^{14}C and ^{3}H Labelled 6-Nitro-7-sulfamoylbenzo[F]quinoxaline-2,3-dione. *J. Labelled Compd. Radiopharm.* **1992**, *31*, 365–373.

(25) Bellamy, F. D.; Ou, K. Selective Reduction of Aromatic Nitro Compounds with Stannous Chloride in Non Acidic and Non Aqueous Medium. *Tetrahedron Lett.* **1984**, *25*, 839–842.

(26) Gillespie, H. B.; Spano, F.; Graff, S. Synthesis of Some Substituted Benzimidazoles, Benzotriazoles and Quinoxalines. *J. Org. Chem.* **1960**, *25*, 942–944.

(27) Landquist, J. K. Quinoxaline *N*-Oxides. Part I. The Oxidation of Quinoxaline and its Bz-Substituted Derivatives. *J. Chem. Soc.* **1953**, 2816–2821.

(28) (a) Bird, C. W.; Cheeseman, G. W. H.; Sarsfield, A. A. 2,1,3-Benzoselenadiazoles as Intermediates in o-Phenylenediamine Synthesis. *J. Chem. Soc.* **1963**, 4767–4770. (b) Tian, W.; Grivas, S. Synthesis of 6-Halo-5-nitroquinoxalines. *J. Heterocycl. Chem.* **1992**, *29*, 1305–1308. (c) Tian, W.; Grivas, S.; Olsson, K. Nitration of 5-Fluoro-2,1,3-benzoselenadiazoles, and the Synthesis of 4-Fluoro-3-nitro-, 4-Fluoro-6-nitro-, 5-Fluoro-3-nitro-o-phenylenediamines and 3,4-Diamino-2-nitrophenols by Subsequent Deselenation. *J. Chem Soc., Perkin Trans. 1* **1993**, 257–261.

(29) Mitchell, R. H.; Lai, Y.-H.; Williams, R. V. N-Bromosuccinimide-dimethylformamide: A Mild, Selective Nuclear Monobromination Reagent for Reactive Aromatic Compounds. *J. Org. Chem.* **1979**, *44*, 4733.

(30) Kher, S. M.; Cai, S. X.; Weber, E.; Keana, J. F. W. Regiospecific Oxidative Nitration of 3,4-Dihydro-6,7-disubstituted Quinoxaline-2(1*H*)-ones Gives 1,4-Dihydro-5-nitro-6,7-disubstituted Quinoxalin-2,3-diones, Potent Antagonists at the NMDA/Glycine Site. *J. Org. Chem.* **1995**, in press.

(31) Silverstein, R. M.; Bassler, G. C.; Morrill, T. C. *Spectrometric Identification of Organic Chemistry*; John Wiley: New York, 1981; p 236.

(32) (a) Leonard, J. P.; Kelso, S. R. Apparent Desensitization of NMDA Responses in *Xenopus* Oocytes Involves Calcium-dependent Chloride Current. *Neuron* **1990**, *4*, 53–60. (b) Williams, K. Ifenprodil Discriminates Subtypes of the *N*-Methyl-D-aspartate Receptor: Selectivity and Mechanisms at Recombinant Heteromeric Receptors. *Mol. Pharmacol.* **1993**, *44*, 851–859.

(33) Gundersen, C. B.; Miledi, R.; Parker, I. Glutamate and Kainate Receptors Induced by Rat Brain Messanger RNA in *Xenopus* Oocytes. *Proc. R. Soc. London B Biol. Sci.* **1984**, *221*, 127–143.

(34) Randle, J. C. R.; Guet, T.; Bobichon, C.; Moreau, C.; Curutchet, P.; Lambolez, B.; de Carvalho, L. P.; Cordi, A.; Lepagnol, J. M. Quinoxaline Derivatives: Structure-Activity Relationships and Physiological Implications of Inhibition of *N*-Methyl-D-aspartate and Non-*N*-methyl-D-aspartate Receptor-Mediated Currents and Synaptic Potentials. *Mol. Pharmaacol.* **1992**, *41*, 337–345.
(35) (a) Woodward, R. M.; Huettner, J. E.; Guastella, J.; Keana, J. F. W.; Weber, E. *In Vitro* Pharmacology of ACEA-1021 and ACEA-1031: Systemically Active Quinoxalinediones with High Affinity and Selectivity for *N*-Methyl-D-aspartate Receptor Glycine Sites. *Mol. Pharmacol.* **1995**, *47*, 568–581. (b) Woodward, R. M.; Huettner, J. E.; Tran, M. T.; Guastella, J.; Keana, J. F. W.; Weber, E. Pharmacology of ACEA-1011: A Novel Systemically Active Ionotropic Glutamate Receptor Antagonist. *J. Pharmacol. Exp. Ther.* **1995**, in press.
(36) Leff, P.; Dougall, I. G. Further Concerns over Cheng-Prusoff Analysis. *Trends Pharmacol. Sci.* **1993**, *14*, 110–112.
(37) Sheardown, M. J.; Neilsen, E. O.; Hansen, A. J.; Jacobsen, P.; Honore, T. 2,3-Dihydroxy-6-nitro-7-sulfamoyl-benzo(*f*)quinoxaline: A Neuroprotectant for Cerebral Ischemia. *Science (Washington, D.C.)* **1990**, *247*, 571–574.
(38) Sheardown, M. J.; Suzdak, P. D.; Nordholm, L. AMPA, But Not NMDA, Antagonism is Neuroprotective in Gerbil Global Ischemia, Even When Delayed 24h. *Eur. J. Pharmacol.* **1993**, *236*, 347–353.
(39) Warner, D. S.; Martin, H.; Ludwig, P.; McAllister, A.; Keana, J. F. W.; Weber, E. In vivo Models of Cerebral Ischemia: Effects of Parenterally Administered NMDA Receptor Glycine Site Antagonists. *J. Cereb. Blood Flow Metab.* **1995**, *15*, 188–196.
(40) Marek, P.; Weber, E. Unpublished results.
(41) Brooke, G. M.; Burdon, J.; Tatlow, J. C. Aromatic Polyfluorocompounds. Part VII. The Reaction of Pentafluoronitrobenzene with Ammonia. *J. Chem. Soc.* **1961**, 802–807.
(42) Sawicki, E.; Carr, A. Structure of 2,1,3-Benzoselenadiazole and Its Derivatives. I. Ultraviolet-Visible Absorption Spectra. *J. Org. Chem.* **1957**, *22*, 503–506.
(43) Chomczynski, P.; Sacchi, N. Single-step Method of RNA Isolation by Acid Guanidinium-thiocyanate Phenol-chloroform Extraction. *Anal. Biochem.* **1987**, *162*, 156–159.
(44) Woodward, R. M.; Polenzani, L.; Miledi, R. Effects of Steroids on γ-Aminobutyric Acid Receptors Expressed in *Xenopus* Oocytes by Poly(A)$^+$ RNA from Mammalian Brain and Retina. *Mol. Pharmacol.* **1992**, *41*, 89–103.
(45) St. Clair, R. L.; Thibault, T. D. Quinoxaline Compounds as Hypnotic Agents. U.S. Patent 3,962,440, 1976.
(46) Dandegaonker, S. H.; Mesta, C. K. Quinoxaline Sulfonamides. *J. Med. Chem.* **1965**, *8*, 884–886.
(47) Allison, C. G.; Chambers, R. D.; Macbride, J. A. H.; Musgrave, W. K. R. Polyfluoroheterocyclic Compounds Part XX. Preparation and Nucleophilic Substitution of Hexafluoroquinoxaline. *J. Fluorine Chem.* **1971/2**, *1*, 59–67.

JM950359B